(Looking) Back to the Future: A reconstruction of historic land use and its application for global change research

Klein Goldewijk, C.G.M.

2012

document version
Publisher's PDF, also known as Version of record

Chapter 6

Applications II: Holocene carbon emissions as a result of anthropogenic land cover change

This chapter has been published as:

Kaplan, J. O., Krumhardt, K. M., Ellis, E. C., Ruddiman, W. F., Lemmen, C. & Klein Goldewijk, K. (2011) Holocene carbon emissions as a result of anthropogenic land cover change. The Holocene, 21, 775-791.

Abstract

Humans have altered the Earth's land surface since the Paleolithic mainly by clearing woody vegetation first to improve hunting and gathering opportunities, and later to make space for agricultural cropland. In the Holocene, agriculture was established on nearly all continents and led to widespread modification of terrestrial ecosystems. To quantify the role that humans played in the global carbon cycle over the Holocene, we developed a new, annually resolved inventory of anthropogenic land cover change from 8000 years ago to the beginning of large-scale industrialization (AD 1850). This inventory is based on a simple relationship between population and land use observed in several European countries over preindustrial time. Using this dataset, and an alternative scenario based on the HYDE 3.1 land use database, we forced the LPJ Dynamic Global Vegetation Model in a series of continuous simulations to evaluate the impacts of anthropogenic land cover change on terrestrial carbon storage during the preindustrial Holocene. Our model setup allowed us to quantify the importance of land degradation caused by repeated episodes of land use followed by abandonment. By 3 ka BP, cumulative carbon emissions caused by anthropogenic land cover change in our new scenario ranged between 84 and 102 Pg, translating to ca. 7 ppm of atmospheric CO_2. By AD 1850, emissions were 325-357 Pg in the new scenario, in contrast to 137-189 Pg when driven by HYDE. Regional events that resulted in local emissions or uptake of carbon were often balanced by contrasting patterns in other parts of the world. While we cannot close the carbon budget in the current study, simulated cumulative anthropogenic emissions over the preindustrial Holocene are consistent with the ice core record of atmospheric $\square^{13}CO_2$ and support the hypothesis that anthropogenic activities led to the stabilization of atmospheric CO_2 concentrations at a level that made the world substantially warmer than it otherwise would be.

6.1. INTRODUCTION

Several attempts have been made to reconstruct the history of anthropogenically-induced land cover change (ALCC), and in some cases the resulting CO_2 emissions, both in the industrial era and in preceding centuries (Ramankutty & Foley, 1998; Houghton et al., 1999; Ramankutty & Foley, 1999; Klein Goldewijk, 2001; Houghton, 2003; Pongratz et al., 2008; Strassmann et al., 2008). Because most countries lack reliable land use surveys prior to the middle of the 20th century, these reconstructions rely on hindcasting techniques based on estimated historical populations and assumptions about how people used the land. A

common hindcasting method, linear scaling, first establishes the quantitative link between modern populations and land use data (typically within the interval 1960-2005) and then uses prior (historical) population data to estimate past land use by assuming near-constant land use per person (Klein Goldewijk, 2001; Pongratz et al., 2008; Klein Goldewijk et al., 2010; Klein Goldewijk et al., 2011).

Land use estimates based on this assumption inevitably show little human land use prior to the exponential population explosion that began near AD 1500 and accelerated through the present day (Figure 1). This finding has led to the conclusion that forest clearance by humans could not have played a significant role in the gradual rise of CO_2 concentrations that began during the middle Holocene about 8 ka (cal. BP; 8000 yr before AD 1950). Atmospheric CO_2 increased by ~22 ppm from the 8k minimum to the start of the industrial era (Ruddiman, 2007).

The assumption that land use per capita has remained constant over time is not supported by published evidence or by widely accepted land use theory. Archeologists, paleoecologists, paleobotanists, anthropologists, and other field-based researchers have repeatedly shown that from the late Paleolithic to the beginning of widespread industrialization, the first human residents and especially farmers in any region used far more land per person than those after them, and that land use per capita has decreased over time as populations increase, land availability per capita declines, technologies improve, and land use intensifies (e.g. Johnston, 2003; for a review see, e.g., Kaplan et al., 2009; Ruddiman & Ellis, 2009). Indeed, Boserup (1965, 1981) synthesized evidence across field studies to develop the most widely used general model of land use intensification, in which population pressure drives farmers to implement ever-more innovative and labor-intensive methods of extracting more food per unit area farmed, so that land use per capita decreases as population density increases.

Regional historical observations from Europe and China support the theory that land cover change per capita fell sharply over at least the last 2000 years (McEvedy & Jones, 1978; Chao, 1986; Ellis & Wang, 1997; Verheyen et al., 1999; Ruddiman, 2003; Ervynck et al., 2007; Hermy & Verheyen, 2007; Kaplan et al., 2009; Ruddiman & Ellis, 2009; Ruddiman et al., in press). In the earliest and least populated phase of the Holocene, most humans were hunter-gatherers, and practiced a nomadic or semi-sedentary lifestyle (e.g.`, Richerson et al., 2001; Bellwood, 2005; Mazoyer & Roudart, 2006). Under these conditions, forest clearing by fire was extensive, both from fires set intentionally to improve foraging conditions, and by the mere presence of humans with anthropogenic fire and livestock (for a review see Williams, 2008). Once agriculture was established, per capita land use decreased steadily. Ruddiman and Ellis (2009), summarized evidence on population and land clearing to suggest that per capita land use has decreased 10-fold since the mid-Holocene. Likewise, in Lemmen's (2009) model of prehistoric technical and societal changes, per capita land use decreased by a factor of seven from the emergence of agriculture at 11 ka to 3 ka.

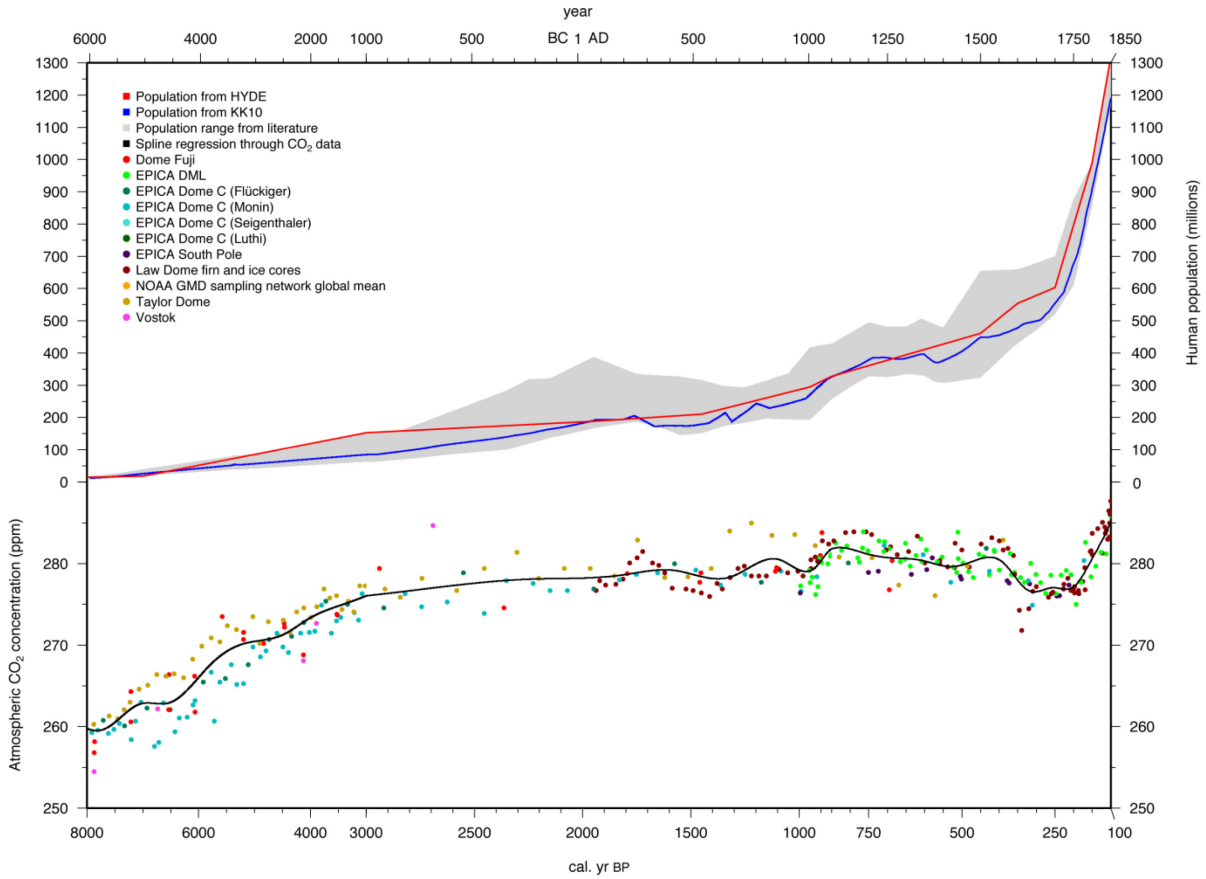

Figure 1. Human population history and record of atmospheric CO_2 concentrations from 8 ka to ad 1850. Time series of population data from 209 regions was used to produce the KK10 ALCC data set. The gray area around the population estimates represents the range of population estimates in literature. The smoothed spline fit to ice core and firn CO_2 records (see Krumhardt and Kaplan, 2010) was used to drive the LPJ DGVM.

In short, the assumption of constant land use per capita in preindustrial times is unjustified. Given that early farmers could have been using more than 10 times as much land per capita as later ones, it is premature to conclude that human activities have played little or no role in the preindustrial (before AD 1850) CO_2 increase (Figure 1). Rather, simulations of preindustrial land use should take into account existing scientific knowledge and theory on how humans are known to have cleared land in the past. Such studies may then provide meaningful tests of the hypothesis that early agriculture caused the unprecedented interglacial CO_2 increases observed 8000 years ago (Ruddiman, 2003; see also Ruddiman et al., in press). Olofsson and Hickler (2008) made a first attempt in this direction, but their study assumed constant per capita land use after 1700, and it lumped earlier clearance into two categories: 90% clearance for 'states and empires', and very little clearance for all other ‘agricultural groups’.

Here we reconstruct carbon emissions caused by ALCC over the Holocene based on contrasting scenarios of population and anthropogenic land use over time, including a new empirical model in which per capita ALCC declines over time and a conventional model that holds per capita ALCC roughly constant over time. These scenarios are used to drive a dynamic global vegetation model (DVGM) to estimate regional and global patterns of changes in terrestrial carbon storage through the last 8000 years. The resulting differences in

global and regional patterns of ALCC and carbon emissions are then contrasted to highlight the global importance of assuming constant land use per capita versus models that incorporate changes in per capita land use with population density. Finally, we discuss how the ALCC emission estimates derived here relate to independent constraints on the global carbon cycle during the Holocene.

6.2. MATERIALS AND METHODS

In order to quantify ALCC emissions over the Holocene we 1) developed a new scenario of global ALCC from 8 ka BP (calendar years before AD 1950) to AD 1850 based on existing methodology, 2) assembled climate, soils and CO_2 data used to drive a Dynamic Global Vegetation Model (DGVM), 3) modified the LPJ DGVM to handle ALCC and made several other small improvements to the model, and 4) ran the model in a number of experiments to characterize the range of possible emissions scenarios. Development of the new ALCC time series involved preparation of a new database of estimates of prehistoric and historical global population. We assembled new driver datasets of CO_2 concentrations and meteorology based on the latest available datasets. The modifications to the LPJ DGVM included a novel mechanism to simulate transient land use and shifting cultivation and an improved geographic distribution of soil organic matter based on compilation of observations. Methods specifically concerning our treatment of ALCC in the DGVM are described below. A detailed description of the rest of our methodology is contained in the supplementary material to this article (see supplementary material at the end of this chapter).

6.2.1 Anthropogenic land cover change (ALCC)

The primary driver of Holocene CO_2 emissions in this study was a gridded time series of global ALCC. We used two ALCC datasets to drive LPJ DGVM, 1) the HYDE 3.1 database (Klein Goldewijk et al., 2010) and 2) a new dataset developed for this study, hereinafter called the Kaplan and Krumhardt 2010 (KK10) dataset. The KK10 scenario makes the central assumption that humans use land more intensively in all regions of the world with increasing population density and land scarceness (Boserup, 1965). In contrast, the standard version of the Historical Database of the Global Environment (HYDE Klein Goldewijk et al., 2010), is based on a nearly linear relationship between population and area of land under agriculture, and shows very little variation in per capita land use. Here, we use the HYDE 3.1 dataset of ALCC (crop + pasture fractions) to provide a comparison to our results with the KK10 scenario and in order to compare our results with those from other carbon cycle studies that used the HYDE dataset (e.g., Strassmann et al., 2008). In using HYDE as input to LPJ, we added the crop and pasture fractions of each gridcell and linearly interpolated between each timeslice. As the development and evaluation of the HYDE database is described in detail in another publication (Klein Goldewijk et al., 2010), here we focus the rest of this section on the description of the new KK10 dataset.

An empirical model for simulating past ALCC was recently developed by Kaplan et al. (2009) and applied to Europe for the past 3000 years. We expanded on this method in the current study by expanding the geographic scope to global and the entire time period from 8000 years ago to AD 1850, when the Industrial Revolution began to profoundly alter relationships

between population and land use (Ellis & Ramankutty, 2008). Uniquely, the Kaplan et al. (2009) method is based on a non-linear relationship between population density and land use, which generally translates to a decrease in per capita land use with time, as population densities increase and land use intensification occurs.

Human population is the main input for estimating ALCC using the KK10 model. We assembled a new, annually resolved database of population from 1000 BC to AD 1850 for 212 regions of the world (Figures 1 and S1). A complete description of the methods used to assemble our historical population database may be found in Krumhardt (2010). In summary, our population estimates are based primarily on McEvedy and Jones (1978), replaced or adjusted wherever better data was available. Adjustments to population estimates for Europe are discussed in Kaplan et al. (2009). For the Western Hemisphere before 15th century contact with Europeans, we used updated values from a number of sources, all of which indicated that the McEvedy and Jones (1978) figures were generally at the very low range of estimates (Denevan, 1992; Krumhardt, 2010). Our dataset therefore presents substantially increased population numbers for the pre-Columbian Western Hemisphere over those of McEvedy and Jones (1978). To capture spatial patterns in population changes across China, provincial data from 221 BC to AD 1850 was used (Zhao & Xie, 1988), allowing detailed improvements in population patterns and dynamics without changing total values significantly from McEvedy and Jones (1978). To extend our population time series for each region from 3 ka back to 8 ka, we used a time series of global population simulated by the Global Land Use and Technological Evolution Simulator (GLUES; Wirtz and Lemmen, 2003, Lemmen 2009).

We simulated ALCC based on population data, maps of land suitability for agriculture and pasture, and a simple relationship between population density and preindustrial land use (Kaplan et al., 2009). Time series of population estimates for each population region were transformed into the fraction of land used by people by first calculating population density on arable land within each region and then applying this value to a sigmoidal function that relates population density to the estimated area of land under deforestation. The amount of arable land in any population region is constrained by observationally based estimates of land suitability for cultivation and pasture at the present day (Ramankutty et al., 2002). In this sense, a limitation of our methodology is that we do not account for the way improvements in technology (e.g., irrigation, terracing, or the development of the steel plow) progressively opened up land to agricultural activities through time (Kaplan et al., 2009). While suitability for cultivation is a function of both climate and soil quality (Ramankutty et al., 2002), pasture suitability is determined only by climate, and accounts for areas suitable for grazing livestock as well as for wood harvest for construction or fuel (Kaplan et al., 2009). The spatial distribution of land use is determined by the total amount of land required for any region and time multiplied by the land suitability factor. This method results in maps of land use that display the most suitable land being cleared first, followed by use of increasingly marginal land as population pressure, and thus land required, increases. The population density-forest clearance relationship deteriorates with industrialization, urbanization and trade, and therefore the KK10 dataset covers only the time period from 8 ka to AD 1850. A detailed discussion of the methodology used to simulate ALCC is contained in Kaplan et al. (2009).

Because the original population density-ALCC relationship was developed using observations in Europe, and the potential productivity of land for agriculture and pasture is much higher in tropical regions and lower in boreal regions, it was necessary to add a potential productivity scaling to our population-ALCC model. Without this scaling, simulated ALCC in tropical regions was unrealistically high in prehistoric times, as even prehistoric societies were able to gain far higher yields in the tropics, even practicing double and sometimes triple cropping (Wilken, 1971; Mathey & Gurr, 1983). We used a high-resolution (5 arc-minute) map of potential Net Primary Productivity (NPP) for the mid-20th century produced by the BIOME4 vegetation model (Kaplan, 2001) to rescale ALCC according to the potential productivity of land using the equation:

$$ALCC = ALCC\ (1.5 - NPP/1400) \quad | \ NPP > 700\ g\ m^{-2}\ yr^{-1} \ | . \qquad (1)$$

NPP is on average roughly twice as high in the most productive areas of the world (NPP ~1400 g m-2 yr-1) than it is in most of Europe (~700 g m-2 yr-1). To avoid underestimating ALCC in cool-temperate and boreal regions, and because these regions are not typically intensively exploited for agriculture in any case, this equation was applied only in areas with NPP exceeding the European average of 700 g m-2 yr-1 (Kaplan, 2001).

The LPJ DGVM was run on a half-degree (30 arc-minute) grid, while both ALCC datasets have a native resolution of 5 arc-minutes. To prepare the ALCC datasets for the DGVM, we averaged each 6 x 6 block of 5' gridcells to the 30' grid used for LPJ.

6.2.2 Other driver data for terrestrial carbon cycle modeling

The LPJ DGVM is driven by spatially and temporally explicit datasets of climate, soil properties and atmospheric CO_2 concentrations (Sitch et al., 2003). As the primary purpose of this study is to quantify the role of ALCC on the terrestrial carbon cycle, and because realistic global paleoclimate forcing datasets are currently neither available from climate models nor based on proxy reconstructions, we used a standard 20th century, observation-based climate dataset to run LPJ: a 100-year long time series of global climate (monthly mean temperature and cloud cover, monthly total precipitation) gridded at 30' resolution.

CO_2 forcing data for LPJ was produced by compositing Antarctic ice-core, firn air, and recent atmospheric measurement records of atmospheric CO_2 concentrations over the Holocene using a regression spline method weighted by the precision of the individual measurements (Krumhardt & Kaplan, 2010). The resulting annual timeseries of CO_2 concentrations was used to drive the LPJ DGVM.

6.2.3 Model configuration for ALCC simulations

To model the effects of ALCC terrestrial vegetation in LPJ, we followed the approach of Strassmann et al. (2008), where managed and unmanaged land is represented on separate sub-grid scale tiles. We made the additional modification of explicitly simulating unmanaged land that was previously under land use, i.e., abandoned land. Thus, our LPJ model setup includes simultaneous simulation of up to three tiles in every 30' pixel: 1) unmanaged land that has never been managed, 2) land under human land use, and 3) abandoned, recovering

land. ALCC fractions are input on an annual time step and unmanaged land is always converted to land use preferentially before abandoned land is reused. Following Strassmann et al. (2008), conversion to agricultural land use (land clearance) from either the natural vegetation or the abandoned tile results in the transfer of all leaf biomass to the litter pool, immediate oxidation of 25% of the aboveground woody biomass, and redistribution of the rest of the wood to two product pools with exponential decay constants of 2 and 20 years, respectively. With land clearance, all living belowground biomass enters the litter pool immediately, and decays or is transferred to soil organic matter following Sitch et al. (2003). Even after conversion to agricultural land, a significant amount of the carbon in the ecosystem may remain in situ, mainly in the form of soil organic matter (for more details on the simulation of soil organic matter dynamics, see section 1.3 of the supplementary methods for this paper). Following initial clearance of the agricultural land use tile, all woody PFTs are prevented from further establishment.

To incorporate shifting land use practices in our ALCC model, we further created a scheme for modeling the turnover of agricultural land that simulates progressive use, abandonment, and conversion of unused land, e.g., shifting cultivation. In this scheme, a land "turnover-time" (tt) is specified in the model run options where 1/tt equals the fraction of the total area under human land use that is simultaneously abandoned and cleared at each annual time step. The total area under human land use at any given time is the same in all simulations, regardless of turnover time, though in simulations where tt is prescribed, a significant fraction of the gridcell can be in the abandoned tile. We defined an unusable fraction of each gridcell as 1 - usable fraction, which is based on climate data and unique to each gridcell (Kaplan et al., 2009; Ramankutty et al., 2002). The unusable fraction always remains under natural vegetation, regardless of the turnover rate. For the simulations with the HYDE land use data, if the fraction of land under anthropogenic land use becomes greater than the calculated usable fraction, then the unusable fraction is reduced to reflect the remaining unused portion. We made experiments specifying turnover of agricultural land with 25-, 50- and 100-year rotation times, in which 4%, 2% or 1% of the land used is turned over annually on all gridcells with ALCC, respectively. Though people in the tropics often implemented shorter rotation times (Cook, 1921; Reina, 1967), performing runs on a global scale with 5-10 year agricultural rotation times would result in the same overall trends in carbon emissions we describe below but with unreasonably high absolute emissions, especially considering that farmers in temperate regions often cultivated the same plots of land continuously (Mazoyer & Roudart, 2006). We further ran a series of experiments as a control scenario where no land turnover is specified, i.e., agricultural land use was permanently established on the same fraction of the gridcell for the duration of the model run.

Model experiments were performed with the LPJ DGVM to simulate the ALCC effects on the carbon cycle over the Holocene. Each run is initialized with a 1000 year spinup period – the SOM pools are analytically equilibrated after 750 years following Sitch et al. (2003) – and then starts at 8 ka and continues to AD 1850, a transient run of 7901 years.

6.3. RESULTS

6.3.1 Scenarios of ALCC

The two ALCC scenarios used in this study differ substantially (Table 1; Figures 2, 3, and S3). In general, the KK10 scenario, in which land use per capita declines as population density increases, consistently produces higher levels of preindustrial ALCC than the HYDE database (Klein Goldewijk et al., 2010), which uses a relatively constant relationship between land use and population similar to mid-20th century levels. Additionally, in KK10, ALCC is more widely distributed within regions with high agricultural suitability, while HYDE generally depicts smaller, more concentrated areas of land clearance, probably because it uses a number of factors in addition to the climate and soil indicators used in KK10, including the location of urban areas, slope, and distance to water bodies (Klein Goldewijk et al., 2010). The slight increase in per capita land use with time seen in HYDE (Figure 2) reflects the country-level trends in per capita land use observed during the late 20th century upon which this dataset is based. Over this time period, both increases and decreases in per capita land use are observed as a result of industrialization and technology, offset by development of export crops and increases in the area of irrigated farmland. Extrapolation of these trends to the past is generally unrealistic.

Table 1. Percent of global land areas under ALCC for the KK10 scenario (this study) and the HYDE 3.1 database (Klein Goldewijk et al., 2011)

		% global land under ALCC		km^2 (millions) under ALCC	
Year	cal. yr BP	KK10	HYDE 3.1	KK10	HYDE 3.1
6050 BC	8000	1.3	0.015	1.86	0.021
1050 BC	3000	6.1	1.2	8.71	1.70
50 BC	2000	9.5	1.9	13.6	2.81
AD 100	1850	10.1	2.0	14.4	2.93
AD 500	1450	10.7	1.9	15.3	2.78
AD 950	1000	12.6	2.3	18.0	3.38
AD 1473	477	16.1	3.5	23.0	5.10
AD 1600	350	15.1	4.3	21.6	6.24
AD 1850	100	20.7	9.9	29.4	14.4

In the HYDE database, a nearly pristine world existed until 3 ka when clearing in northeast China, the Middle East, Europe and South America began to emerge (Table 1; Figure 3a). In contrast, the KK10 land use scenario simulates that these regions, in addition to parts of the Indian subcontinent and Mesoamerica, were up to 40% under human land use at this time period. 2000 years later, by AD 1, ALCC only slightly increases in the HYDE dataset, while in the KK10 scenario, lands of the Middle East and Indian regions were nearly 70% exploited. Moreover, the KK10 scenario shows that parts of Mesoamerica, the Andes, Europe and China were nearly 60% cleared and some parts of sub-Saharan Africa were up to 50% cleared at AD 1.

From AD 1500 to AD 1600 a decrease in anthropogenic land use in the Western Hemisphere is visible in both datasets, as the indigenous populations of the Americas succumbed to disease and war brought by European explorers and colonists (Figure 3b). The collapse of

large pre-contact populations with advanced agriculture, which were especially concentrated in Mesoamerica and the Andes, led to high amounts of land abandonment in the KK10 dataset. The low levels of ALCC shown at AD 1500 in the HYDE scenario are almost entirely abandoned 100 years after conquest.

By AD 1800, anthropogenic land use in the Americas accelerated with the spread of colonies and nations founded by Europeans. The KK10 scenario shows the northeast United States and the eastern coast of Brazil to be 40% to 50% under agriculture by AD 1850. The HYDE dataset shows only limited patches of land clearance over the eastern half of the United States, and no ALCC in eastern South America. There is also disagreement between ALCC datasets at this time period in Southeast Asia, Eastern Europe and the Middle East, where substantially more ALCC is depicted in the KK10 scenario. At AD 1850, the KK10 scenario simulates ~21% of global land area (29.4x106 km^2) experiencing ALCC, while in the HYDE scenario only 10% (14.4x106 km2) of land is used (Table 1; Figure S3).

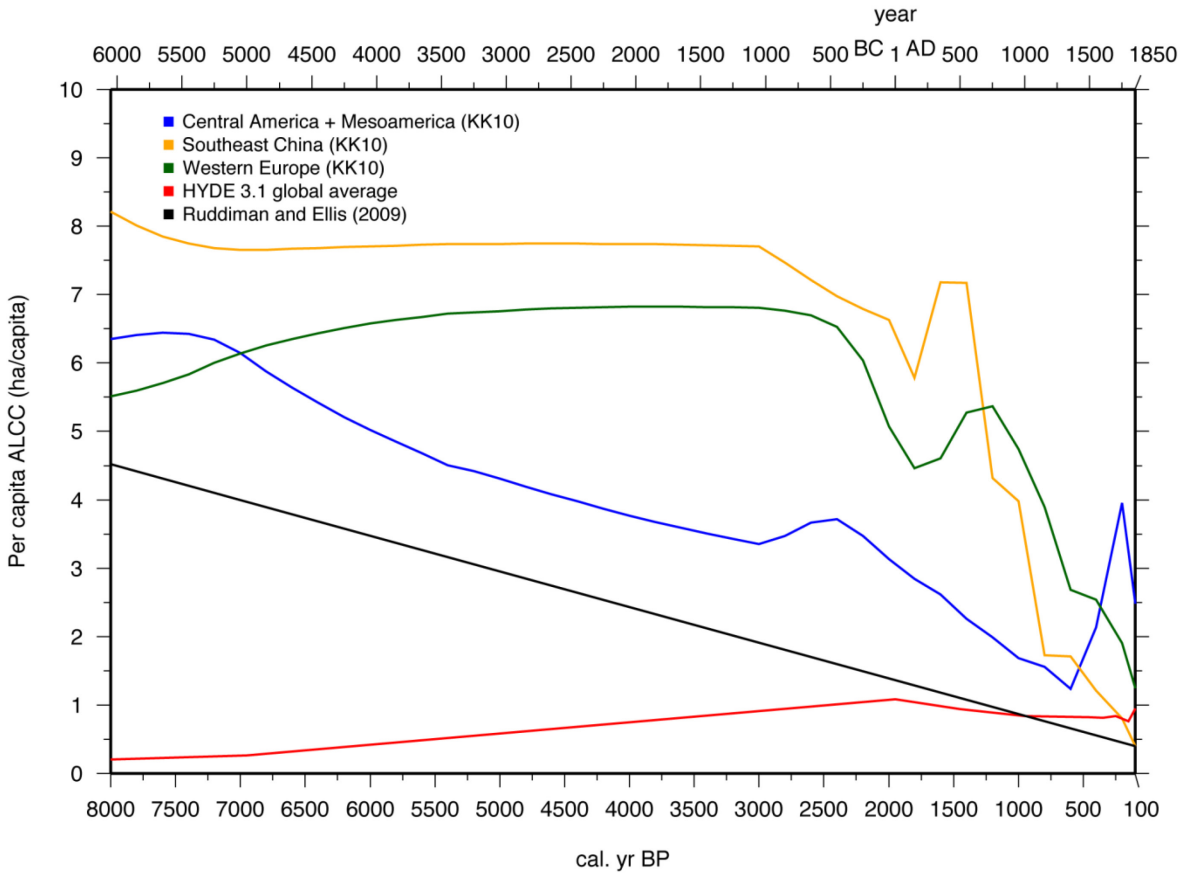

Figure 2. Per capita ALCC from 8 ka to ad1850 for western Europe (average of Italy, Spain, France, and Germany), southeast China (average of the provinces Fujian, Guangdong, Jiangsu, Jiangxi, Zhejiang, and Anhui), and the Mesoamerica-Central America regions from the KK10 scenario, as well as global per capita ALCC from HYDE 3.1 data base and from Ruddiman and Ellis (2009).

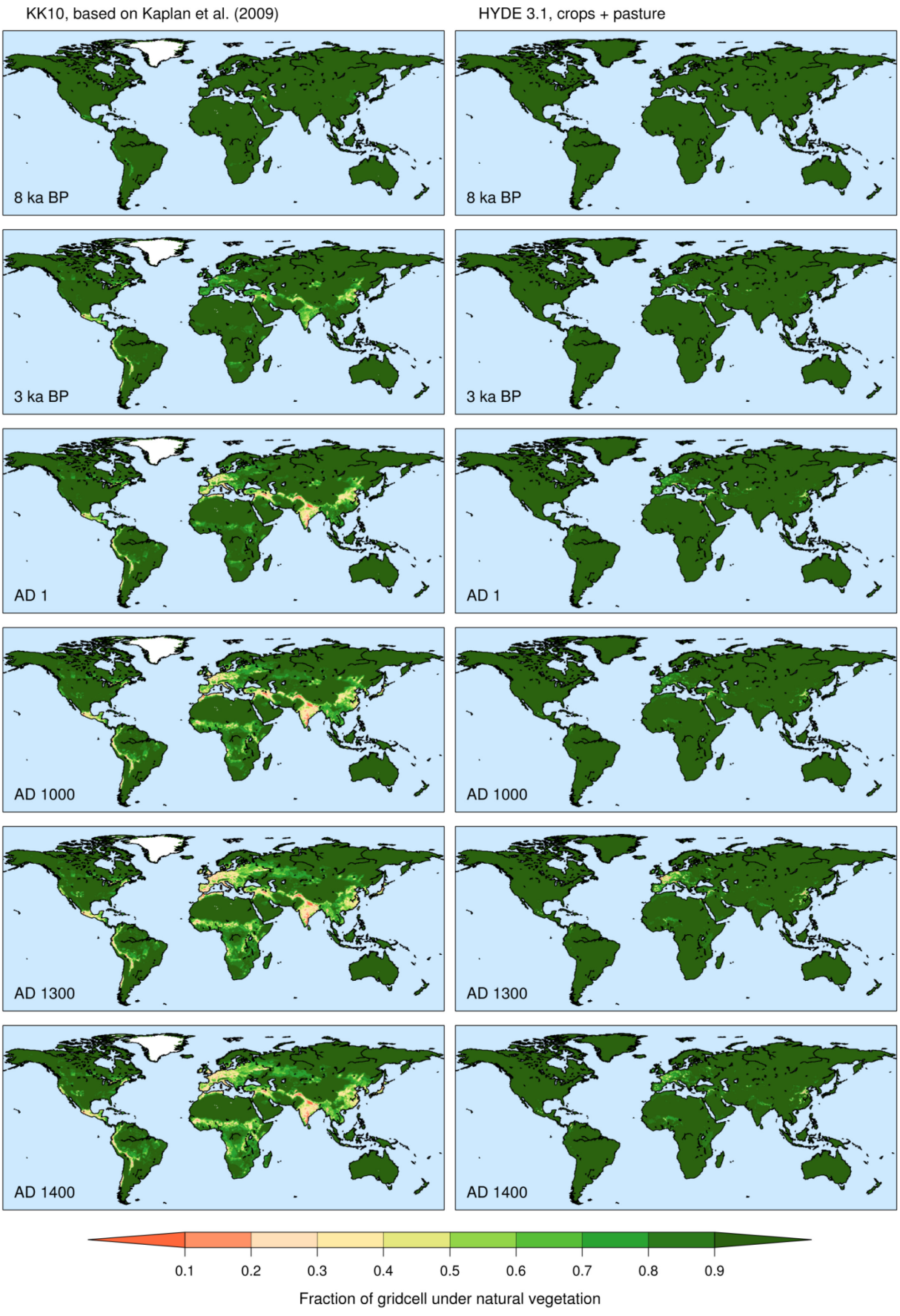
KK10, based on Kaplan et al. (2009)
HYDE 3.1, crops + pasture
8 ka BP
8 ka BP
3 ka BP
3 ka BP
AD 1
AD 1
AD 1000
AD 1000
AD 1300
AD 1300
AD 1400
AD 1400
0.1
0.2
0.3
0.4
0.5
0.6
0.7
0.8
0.9
Fraction of gridcell under natural vegetation

.

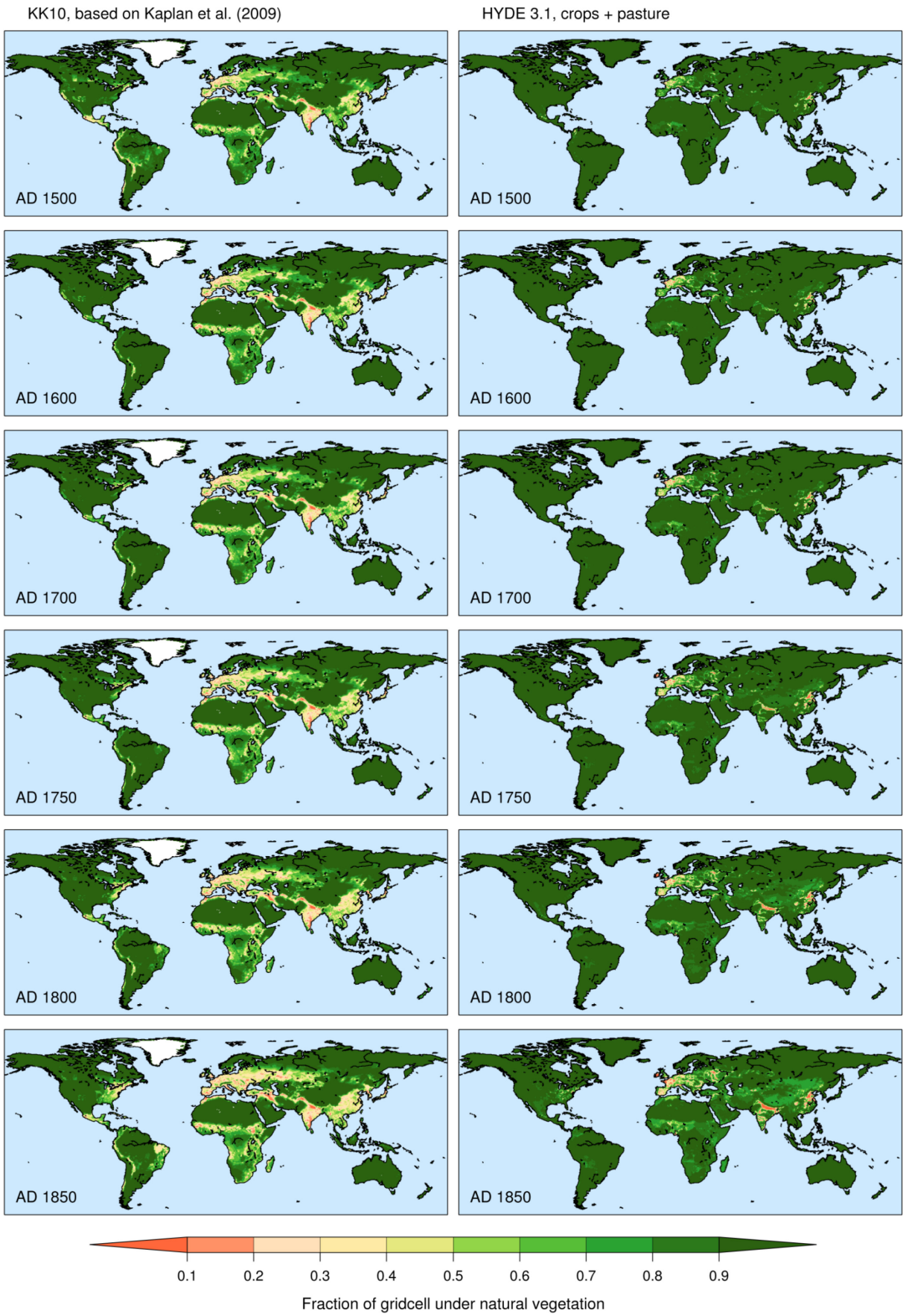

Figure 3. ALCC maps comparing the two scenarios used in this study, KK10 and HYDE 3.1, depicting the fraction of each gridcell under natural vegetation for the timeslices (a) 8 ka BP, 3 ka BP, ad 1, ad 1000, ad 1300, and ad 1400, and (b) ad 1500, ad 1600, ad 1700, ad 1750, ad 1800, and ad 1850.

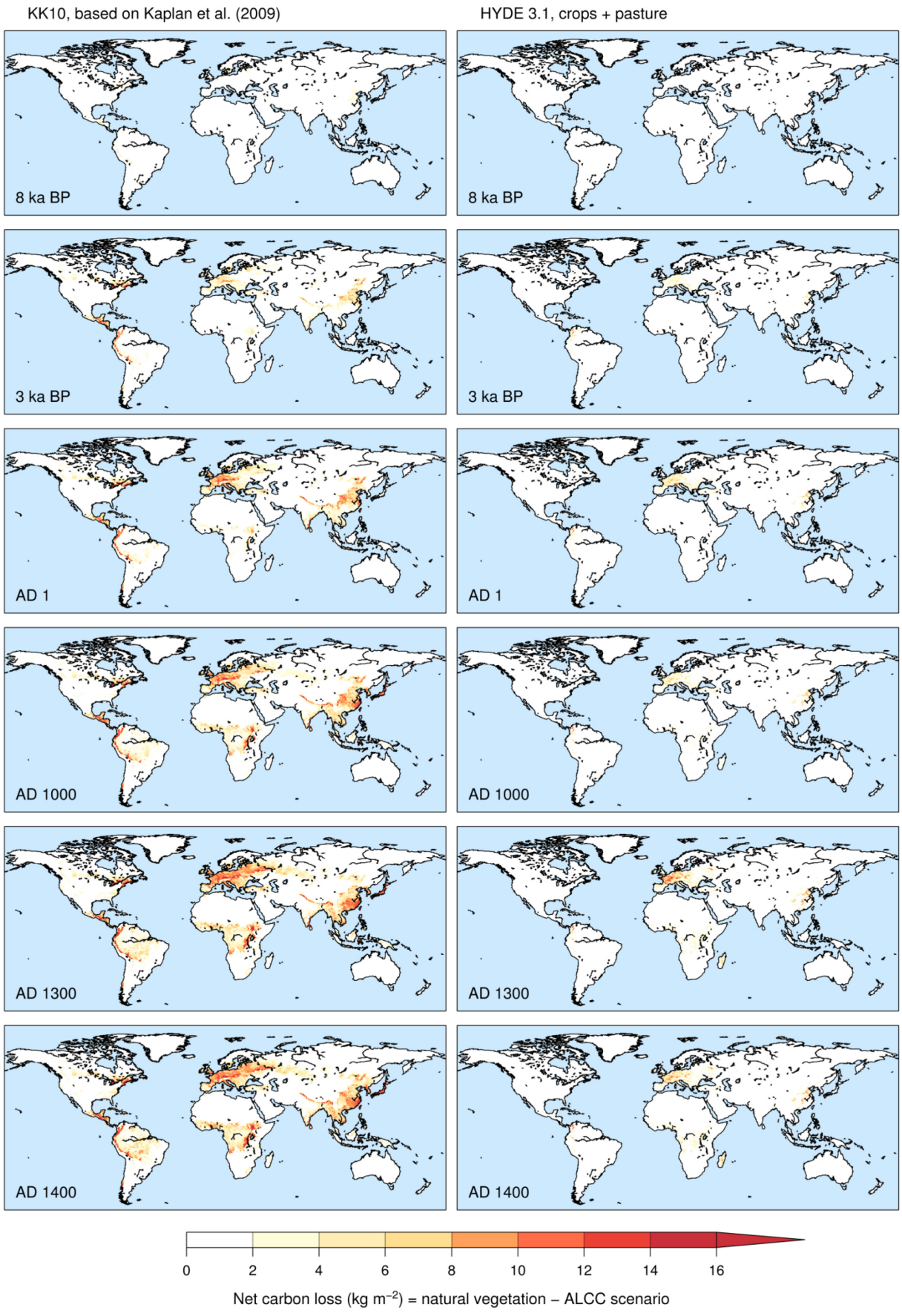
KK10, based on Kaplan et al. (2009)
HYDE 3.1, crops + pasture
8 ka BP
8 ka BP
3 ka BP
3 ka BP
AD 1
AD 1
AD 1000
AD 1000
AD 1300
AD 1300
AD 1400
AD 1400
0
2
4
6
8
10
12
14
16
Net carbon loss (kg m^{-2}) = natural vegetation – ALCC scenario

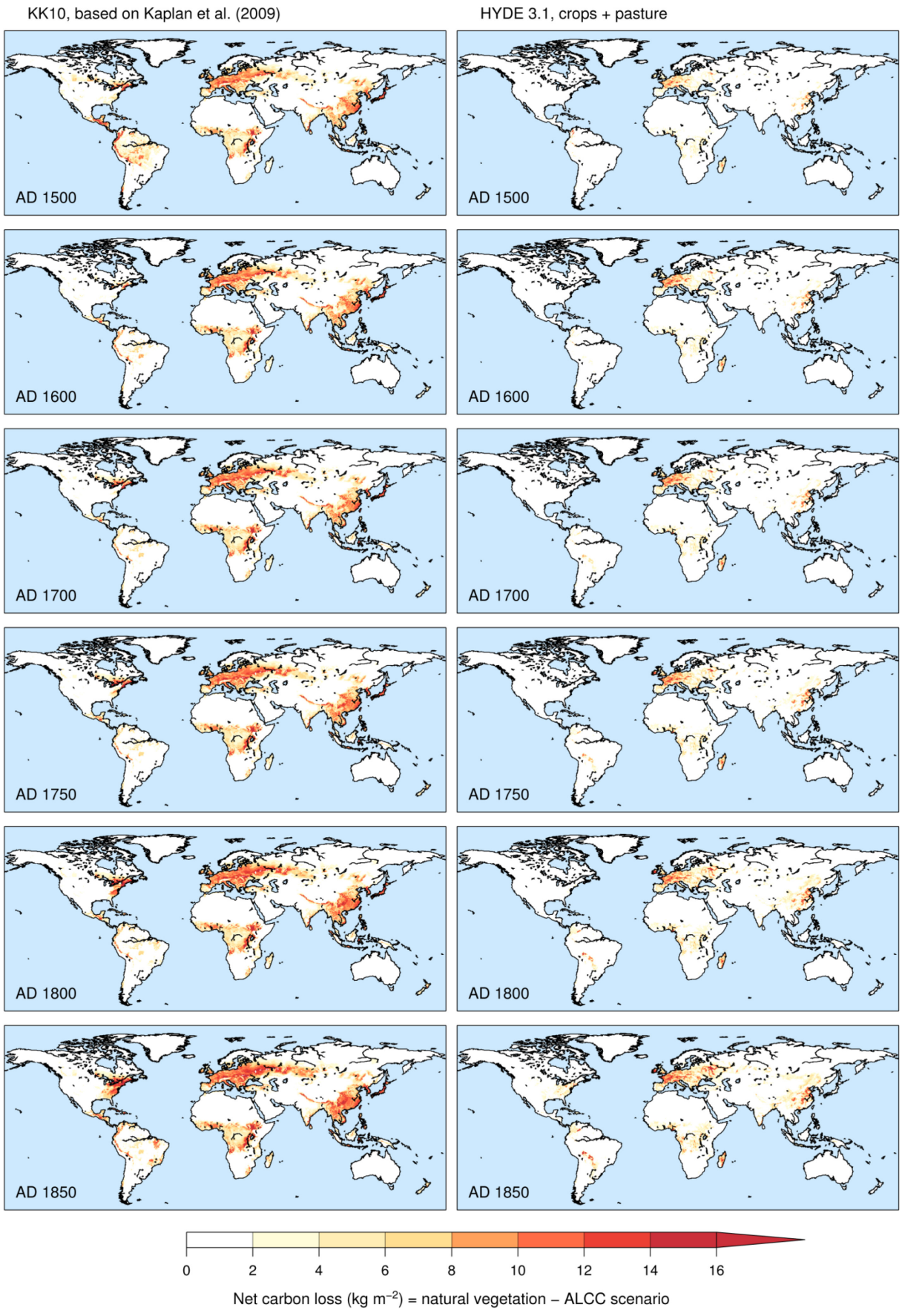

Figure 4. Maps of the difference in LPJ-simulated total terrestrial carbon storage between the ALCC scenarios and control run. Maps are for the same timeslices as those depicted in Figure 3.

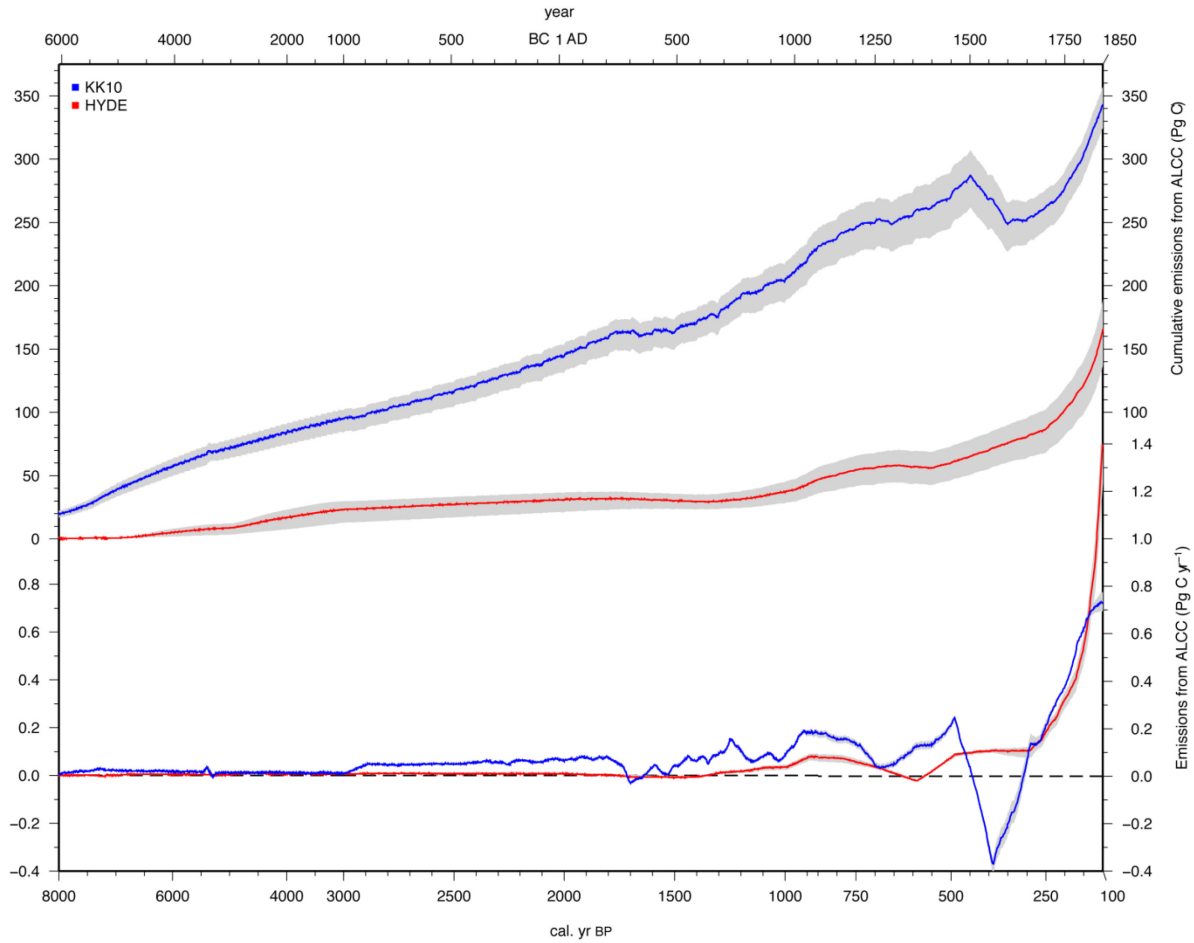

Figure 5. Cumulative carbon emissions (top; Pg C) and annual emissions (bottom; Pg C/yr) from ALCC resulting from LPJ DGVM runs using the KK10 and HYDE ALCC scenarios. The shaded gray area is represents the range from runs with 25- and 100-year agricultural rotations and no rotation, while the colored lines represent runs with a 50-year agricultural rotation.

6.3.2 Geographic distribution of changes in carbon storage

The amount of carbon emitted from ALCC in a region strongly depends on the vegetation that would exist there naturally. For example, at AD 1 on the Indian subcontinent, high levels of ALCC correspond with low levels of carbon loss in the southern part of the continent dominated by grassland or savanna, while lower levels of ALCC result in much greater carbon loss in the humid forest areas along southern foothills of the Himalaya (Figures 3a and 4a). Likewise, the relatively small amounts of ALCC in the densely forested landscapes around the St. Lawrence Valley of North America and in Mesoamerica led to high amounts of carbon emissions as a result of ALCC (Figures 3 and 4; KK10 scenario). In the HYDE scenario, in all time periods, only Europe stands out as a significant source of carbon emissions from ALCC (Figure 4a and b). In this scenario, other areas of the world, such as China and the Americas, only start to result in substantial amounts of ALCC emissions during the last centuries of the model run.

6.3.3 Global trends in carbon storage over the Holocene

The large dissimilarity between the ALCC datasets is reflected in the time series of anthropogenic carbon emissions produced by the DGVM for each scenario. In Figure 5 the difference in terrestrial carbon storage between the ALCC scenarios and control run (with no ALCC) is presented. Cumulative carbon emissions from ALCC by AD 1850 range from 137 to 189 Pg (1 Pg = 1 Gt) for the HYDE dataset and from 325 to 357 Pg C for the KK10 dataset, depending on the land turnover time (Figure 5; Table 2). The effect of CO_2 fertilization is shown in Figure S2 as living biomass increased concurrently with the slow rise of CO_2 during the Holocene for the control scenario.

Generally, HYDE-based simulations show that the majority of ALCC carbon emissions occurred during 500 years prior to industrialization, whereas in the KK10 scenario emissions from ALCC are more gradual and show significance beginning at 8 ka. As a result, cumulative emissions caused by preindustrial ALCC are much lower in the HYDE scenarios as compared to the KK10 scenarios (Table 3). Additionally, the implementation of ALCC rotation has the effect of increasing emissions slightly, but the overall trend of carbon emissions stays the same (Table 2; Figure 5). As the carbon emissions resulting from a land use rotation of 50 years results in emissions that are intermediate between no rotation (continuous cultivation of the same plot of land) and a 25 year rotation time, we describe these results here as our standard scenario.

Table 2. Cumulative carbon emissions from ALCC (Gt C) for the KK10 and HYDE ALCC scenarios for 25, 50, and 100-year agricultural rotations and no rotation

Year	Cal. yr BP	ALCC emissions (Pg C)							
		KK10				HYDE 3.1			
		25-yr rotation	50-yr rotation	100-yr rotation	No rotation	25-yr rotation	50-yr rotation	100-yr rotation	No rotation
6050 BC	8000	22	20	18	17	0	0	0	0
1050 BC	3000	102	95	90	84	30	23	19	13
50 BC	2000	154	145	139	132	36	31	27	21
AD 100	1850	166	156	150	143	37	32	28	23
AD 500	1450	179	169	162	155	35	30	26	24
AD 950	1000	218	204	196	187	45	37	33	28
AD 1473	477	298	279	267	254	76	62	55	48
AD 1600	350	265	249	239	227	90	76	67	61
AD 1850	100	357	343	334	325	189	166	151	137

LPJ runs using the KK10 dataset compared to the control (natural vegetation) scenario indicate that ALCC emissions prior to 3000 years ago ranged from 84 to 102 Pg C (Table 2, Figure 5). However, when using the HYDE scenario, LPJ simulates only 13 to 30 Pg carbon emissions due to ALCC over this entire time period. The HYDE scenario appears relatively stable at roughly 30 Pg C cumulative emissions from ALCC (3400 Pg C total in global terrestrial ecosystems; Table 3) from 1000 BC until ~ AD 1000, where emissions from ALCC finally start to increase slightly (Tables 2 and 3; Figure 5). Emissions from ALCC simulated with the KK10 scenario increase continuously from 8000 years ago until roughly AD 200, where there is a 300 year period of stable or slightly decreasing emissions, followed by increasing emissions to ~ AD 1350 where there is another short period of uptake coincident with the Black Death epidemic in Europe. Slight dips in emissions during these two European events are also visible in the HYDE results.

Table 3. Total carbon stocks, carbon in living biomass, litter carbon, and soil carbon in global terrestrial ecosystems (Pg C) for the control scenario (natural vegetation), and the KK10 and HYDE ALCC scenarios for selected timeslices of the LPJ model runs. For the model runs with ALCC, values are means of 25, 50, and 100-year agricultural rotations and no rotation, and the range around the mean is shown in parentheses

Year	Cal. yr BP	Carbon stock (Pg)											
		Control				KK10				HYDE			
		Total	Living biomass	Litter	Soil	Total	Living biomass	Litter	Soil	Total	Living biomass	Litter	Soil
6050 BC	8000	3276	794	338	2144	3257 (6)	782 (8)	336 (0.4)	2138 (2)	3276 (6)	794 (0)	338 (0)	2144 (0)
1050 BC	3000	3396	843	348	2205	3303 (18)	785 (30)	340 (2)	2178 (11)	3374 (18)	833 (8)	347 (0.3)	2194 (10)
50 BC	2000	3411	850	349	2213	3269 (22)	764 (38)	336 (2)	2170 (14)	3382 (22)	834 (11)	346 (1)	2203 (5)
AD 100	1850	3427	846	360	2221	3274 (23)	753 (40)	346 (3)	2175 (14)	3397 (23)	829 (11)	358 (1)	2211 (4)
AD 500	1450	3430	847	360	2223	3263 (24)	746 (44)	345 (3)	2172 (18)	3401 (24)	831 (11)	358 (1)	2212 (1)
AD 950	1000	3420	854	348	2218	3218 (31)	732 (51)	331 (3)	2155 (18)	3384 (31)	835 (12)	346 (1)	2203 (5)
AD 1473	477	3442	853	360	2229	3168 (44)	693 (58)	337 (3)	2137 (11)	3382 (44)	823 (16)	356 (1)	2203 (12)
AD 1600	350	3434	849	359	2226	3189 (38)	711 (55)	337 (3)	2141 (14)	3360 (38)	814 (17)	353 (1)	2194 (14)
AD 1850	100	3426	857	350	2219	3087 (32)	672 (51)	319 (3)	2096 (15)	3266 (32)	785 (24)	337 (2)	2144 (30)

After AD 1350, ALCC emissions increase in the KK10 scenario to AD 1500, when the collapse of indigenous populations in the Western Hemisphere led to widespread land abandonment. The following century between AD 1500 to 1600 is marked by a ~ 40 Pg uptake of carbon into the terrestrial biosphere. Rates of carbon sequestration into the terrestrial biosphere reach more than 0.3 Pg C yr-1 (Figure 5) in the KK10 scenario. No uptake of carbon is evident, at least on a global scale, in the HYDE-based scenarios for this time period (Figure 5). During the last 200 years of our model runs (AD 1650 to 1850) carbon emissions reach similar rates for both ALCC datasets (Figure 5), as total emissions reach 166 Pg C for the HYDE scenario and 343 Pg C for the KK10 scenario. The KK10 scenario runs result in a much higher total preindustrial emissions due to the larger magnitude of prehistoric ALCC emissions.

Table 4 presents preindustrial emissions from ALCC from a number of other studies. The carbon emission numbers derived in this analysis are substantially higher than those from most previous simulations. For the preindustrial era, previous estimates have ranged between 48-153 Pg C, whereas our simulations based on the KK10 and HYDE datasets indicate that releases of 325-357 Pg C and 137-189 Pg C could have occurred, respectively.

Table 4. Preindustrial and Industrial carbon emissions (Pg C) due to ALCC comparing this study with other published results

Land use simulation	Pre-1850
	Pg C
Olson et al. (1983)[a]	240–540
DeFries et al. (1999)[b]	48–57
Strassmann et al. (2008)	94
Olofsson and Hickler (2008)	114
Pongratz et al. (2009)	63
Stocker et al. (2010) (HYDE)	50
Stocker et al. (2010) (X1)	153
Kaplan et al. (this study) (KK10)	325–357
Kaplan et al. (this study) (HYDE)	137–189
Lemmen (2009)	54
$\delta^{13}CO_2$ Mass Balance	
Elsig et al. (2009)	50
Ruddiman et al. (forthcoming)	310–395

[a] Estimate of 'natural vegetation' of a pre-agricultural world minus late twentieth-century vegetation.
[b] Based on conversion of vegetation reconstructions of Matthews (1983) and Leemans and Cramer (1991).

6.4. DISCUSSION

Large differences between the two ALCC datasets in this study highlight the remarkable amount of uncertainty in estimating the magnitude and overall trend of Holocene ALCC. Though both methods rely heavily on population data to estimate ALCC, the <1 ha per capita preindustrial (before AD 1850) values implemented by HYDE result in conservative land use estimates, whereas the nonlinear relationship used to create the KK10 dataset implies a Boserupian view of fast expansion of anthropogenic land use at low population densities, with progressive intensification of land use as population pressure increases (Kaplan et al., 2009; Ruddiman & Ellis, 2009). Per capita land use estimates in KK10 are significantly higher than those of HYDE, with rough estimates by Ruddiman and Ellis (2009) providing a middle ground (Figure 2). The two methods used in this study result in ALCC estimates that are strikingly different (Figure 3), and portray an upper bound (KK10) and a lower bound (HYDE) to the range of uncertainty that exists for Holocene ALCC.

Much of the uncertainty around the extent of past land use comes from the lack of knowledge about the magnitude and distribution of the global human population and the time course of technological evolution and intensification. While global population estimates at 3 ka differ by more than a factor of four (range 50-225 x 106(see, e.g., Dearing, 2006; Boyle et al., 2010), estimates of the level of intensity with which humans use land are also highly uncertain. In the following sections, we discuss our results in the context of previous attempts to quantify Holocene ALCC carbon emissions, both from modeling and top-down estimates and we provide evidence to support our model simulations based on the ice core record of atmospheric CO_2 concentrations and $\delta^{13}CO_2$. Finally we assess the possibility of evaluating our simulations in light of the paleoecological and other proxy records.

6.4.1 Uncertainities and comparisons to other studies

The differences in estimates of preindustrial emissions between the KK10 scenario and other studies (Table 4) result mainly from higher amounts of prehistoric land use simulated in this ALCC scenario, but could also result from a number of other factors, including differences in estimates of the size of past human populations (see, e.g., Boyle et al., this volume), and variability in the carbon density of natural vegetation in regions where natural forests were converted to agriculture. In general, previous estimates of preindustrial carbon emissions from ALCC appear to be substantial underestimates resulting from the assumption that per capita land use has remained constant for the past 8000 years, an assumption not in agreement with observations (Boserup, 1965; Boserup, 1981; Chao, 1986; Ellis & Wang, 1997; Ruddiman & Ellis, 2009; Ruddiman et al., in press).

Dissimilarities between our results using the HYDE land use scenario and other studies based on HYDE (e.g., Strassmann et al., 2008) can be attributed our choice of driver datasets and the modified LPJ setup described in section 2.3. We also used a higher spatial resolution for simulations (0.5°) than some prior HYDE-based studies (e.g., 3.75° x 2.5°; Strassmann et al., 2008), avoiding errors caused by spatial averaging in heterogeneous regions (coastal, mountains, etc.). Our modeling system differentiates between pristine lands and lands recovering from previous ALCC; including this regrowing fraction causes greater carbon emissions earlier in time, as more of the land area is (or has been) under human influence at

any given time. In contrast, our treatment of pastureland use could result in overestimates of ALCC emissions. Here, 100% of woody vegetation is removed on pastureland; leaving residual patches of natural vegetation, e.g., in a low intensity pasture landscape, would result in lower overall emissions, though we expect this effect to be much smaller than the effects of shifting cultivation and progressive land degradation. Also, the updated soil and climate datasets (supplementary methods) used in this study could lead to differences in natural carbon compared with other studies, though these effects are likely to be small over the long time scales considered here (Jung et al., 2007).

A substantial reason for the range of global carbon change estimates is uncertainty in assessing how much carbon is stored in 'natural' vegetation (Olson et al., 1983). For example, an early synthesis by Bazilevich et al. (1971) cites a global value of 1080 Pg in living biomass under conditions undisturbed by humans. A number of more recent modeling studies that ignore preindustrial ALCC resulted in simulations of peak Holocene terrestrial C storage (plants and surface soils) of 1600-2500 Pg (Cramer et al., 2001; McGuire et al., 2001; Kaplan et al., 2002; Sitch et al., 2003), with about one third of total C stored in living biomass. Olson et al. (1983) point out that modern forests are likely to be degraded carbon-poor versions of pristine forests. Of the few "natural" forest patches that remain, most have survived because they were in terrain too remote, steep, or otherwise uneconomical to be cut, and their carbon density would thus be lower than in the more productive lowland soils used first for agriculture and pasture (Ellis & Ramankutty, 2008). Other forests in parks or forest reserves were previously cut and, in the absence of management, would take centuries to recover to a natural state (Hermy & Verheyen, 2007). Still others have been degraded by humans seeking firewood or by frequent incursions of livestock.

Irreversible ecological shifts caused by anthropogenic deforestation, and related changes in regional climate driven by this permanent land cover change, could also influence the Holocene time series of terrestrial carbon storage in a way that is not captured in our current study. Deforestation, followed by soil erosion and land degradation, has been recognized for decades as a potential source of semi-permanent land cover change (Godwin, 1944; Walker, 1966). The possibility that these land cover changes could affect local to regional climate patterns was hypothesized already in Antiquity by Theoprastus (Hughes, 1983). Recent studies confirm the potential of land cover change in influencing regional climate and, through land-atmosphere feedbacks, reinforcing land cover changes that were initially human-induced.

In the summer-monsoon regions of southern Asia, ALCC is hypothesized to have been responsible for a weakening in recycling of moisture by evapotranspiration, and a subsequent reduction in carbon density in the surviving woodland patches (Takata et al., 2009). In the Mediterranean region, ALCC may have also resulted in regional climate changes and shifts from forest to shrubland vegetation even in areas that were later abandoned (Van der Knaap & van Leeuwen, 1995; Dümenil Gates & Ließ, 2001; Grove & Rackham, 2001a; de Beaulieu et al., 2005; Tinner et al., 2009). These effects of land degradation preventing the establishment of climatically potential natural vegetation is not handled in the current modeling study, though all of the abovementioned effects would lead to increased cumulative ALCC emissions over the Holocene. In this sense, our estimates of ALCC emissions may still represent an underestimate, particularly for those regions of the world

where long-term land degradation is observed, e.g., the Mediterranean basin (Grove & Rackham, 2001b).

Aside from sequestration of carbon in peatlands (Yu, 2010), natural changes in terrestrial carbon storage over the Holocene would have been small compared to anthropogenic effects. The expansion and contraction of the Afro-Asian monsoon system did not result in significant afforestation, rather being a dynamic between desert and sparsely vegetated steppe and xerophytic shrubland (Hoelzmann et al., 1998; Brovkin et al., 2002). In other parts of the world, climatic influences on vegetation cover were small (Wanner et al., 2008), and globally terrestrial ecosystems were generally carbon neutral between 8 ka and preindustrial, with respect to climate (Figure S2; Kaplan et al., 2002).

In simulations with the KK10 dataset, a significant uptake of carbon as a result of ALCC (~40 Pg) is observed following European contact with indigenous populations of the Western Hemisphere (ca. AD 1500 to 1600). A study by Pongratz et al. (this volume) rejects the hypothesis that historical events such as the demographic collapse of populations in the Americas substantially impacted atmospheric CO_2, due to 1) delayed temporal dynamics of regrowth, 2) increased soil respiration from past ALCC, 3) continued ALCC in other parts of the world, and 4) counteracting responses of global carbon pools. However, according to the KK10 scenario, Central and South America were already highly deforested by 3 ka (Figure 3), and most of the soil carbon from the original forests would have decomposed long before European contact, especially in the tropics where decomposition is fast (Chambers et al., 2000; Trumbore, 2000). Though forests in temperate regions of North America took longer to recover (Denevan, 1992), in the high productivity regions of tropical America, forest growth progresses quickly, especially during early stages of growth, some species fixing more than 10 tons of carbon ha-1 yr-1 (Riaño et al., 2002; Faust et al., 2006). Lastly, the massive regrowth of these forests would unlikely have been balanced by ALCC in other parts of the world because other areas with high population densities such as Europe and China, were highly deforested and experienced demographic and climatic crises during this period (e.g., the fall of the Ming Dynasty in China, Little Ice Age) which also resulted in periods of afforestation.

6.4.2 The ice core record of Holocene CO_2 and isotope mass balance constraints on ALCC emissions

The ice core record of atmospheric CO_2 concentrations over the Holocene (Figure 1) displays a number of features that may be correlated with changes in the simulated record of ALCC emissions when using the KK10 scenario (Figure 5). Making a direct comparison between these records is incorrect, however, because our model simulations omit other major elements of the global carbon cycle that are known to have changed over the Holocene, including ocean chemistry, coral reefs, and peatlands. Nevertheless it is illustrative to note some of the periods of correspondence between the curves. The KK10 simulations show a rapid increase in ALCC emissions between 8 ka and roughly 3 ka, corresponding with the increase in CO_2 concentrations over this time period. The simulated emissions of up to 100 Pg can explain just under half of the ~15 ppm increase in atmospheric CO_2 over this time period. We cannot directly assess the hypothesis that anthropogenic activities precluded glacial inception in the late Holocene (Ruddiman, 2007) but the ALCC emissions we simulate

would likely have contributed to the increase in CO_2 concentrations during the key time period after 8 ka when insolation forcing favored a return to glacial conditions.

Between 3 ka and about AD 300 (1.75 ka) ALCC emissions continue to rise steadily and at a higher rate compared to the earlier Holocene (Figure 5), while very little variability is observed in atmospheric CO_2 (Figure 1). The small reduction in emissions in AD 300-500 (the Migration Period in Europe) may be correlated with a very small drop in atmospheric CO_2 concentrations around this time. More dramatic is the up to 10 ppm drop in CO_2 concentrations between AD 1500-1700 (MacFarling Meure et al., 2006); this corresponds closely to the time of maximum carbon uptake as a result of land abandonment in the Western Hemisphere following European contact. The ~40 Pg uptake of carbon we simulate during this time period can explain some of the drop in CO_2 concentrations, and lends support to previous hypotheses on this topic (Ruddiman, 2005; Nevle & Bird, 2008).

The carbon-isotope ($\delta^{13}C$) composition of CO_2 in ice-core air bubbles can be used to assess net emissions/storage of terrestrial carbon during previous millennia. Elsig et al. (2009) measured a small negative $\delta^{13}CO_2$ trend of -0.03‰ over the last 7000 years, although one of the two methods they used indicated a larger (~0.09‰) decrease. Based on carbon/CO_2 scaling from simulations with the Bern carbon cycle model (Joos et al., 2004), these $\delta^{13}CO_2$ trends imply net terrestrial carbon emissions of ~40-125 Pg from 7 ka to the start of the industrial era. Allowing for the effects of other natural factors (CO_2 fertilization, monsoon-related releases and storage of carbon, and carbon storage in peat), Elsig et al. (2009) estimated Holocene ALCC emissions of ~50 Pg C. This amount, equivalent to a CO_2 increase of 3.5 ppm, agrees with several of the estimates presented in Table 4. However, the assessment of Elsig et al. (2009) allows for only 40 Pg of carbon storage in boreal peats over the last 7 ka, which has large implications for the allowable amount of ALCC emissions under isotope mass-balance constraints. Several studies suggest that this figure for Holocene peat accumulation could be a significant underestimate.

Bottom-up attempts to estimate the amount of carbon sequestered in peats over the Holocene result in a published range of 250-450 Pg C (Gorham, 1991; Gajewski et al., 2001; MacDonald et al., 2006; Frolking & Roulet, 2007; Yu, 2010). These studies are based on syntheses of basal age of peats and simple to complex process modeling of peatland development. Yu (2010) estimated that ~270 Pg C were stored in boreal peatlands during the last 7000 years, consistent with estimates by Gorham (1991) and Gajewski et al. (2001). Ruddiman et al. (2010) noted that this estimate would leave an unexplained difference of ~310-395 Pg C between the large net burial of carbon in peats and the small net carbon release indicated by the $\delta^{13}CO_2$ signal. The only remaining explanation for this unaccounted-for carbon appears to be anthropogenic emissions. All of the preindustrial estimates listed in Table 4 fall well short of explaining this 310-395 Pg residual except the 325-357 Pg C estimate we made here using the KK10 ALCC scenario as a driver. The small late-Holocene $\delta^{13}CO_2$ decrease that has previously been interpreted as favoring a very small (~50 Pg) input of anthropogenically derived terrestrial carbon during the last 7 ka needs to be re-examined. If almost 300 Pg of terrestrial carbon was sequestered in peatlands over this time period, explaining a net release of ~40-125 Pg of terrestrial carbon requires anthropogenic emissions far larger than the 50 Pg C value used by Elsig et al. (2009).

6.4.3 Evaluation of the ALCC scenarios

The lack of continental- to global-scale syntheses of evidence for human impact on the Earth's land surface makes it difficult at this point to perform anything more than a superficial, qualitative evaluation of our ALCC scenario results. Developing a continuous synthesis of global human impact at the regional level is currently a major focus of interdisciplinary research coordination, e.g., through the AIMES/PAGES IHOPE program. These ongoing efforts should be combined with existing surveys of human impact over the Holocene using multiple proxies (Dearing, 2006; Sugita, 2007a; Sugita, 2007b; Hellman et al., 2008; Gaillard et al., 2010), and with historical and archaeological data syntheses that have traditionally been overlooked by the natural science community (e.g.`, Zimmermann et al., 2004; Weninger et al., 2006). At the site scale, there is considerable paleoecological and archaeological evidence for early extensive human land use in, e.g., Andes (Chepstow-Lustry & Winfield, 2000), Mesoamerica (Pohl et al., 1996), Europe (Tinner et al., 2007), and China (Ren, 2000). While syntheses of charcoal records from remote areas of the globe attribute Holocene trends in biomass burning to climatic changes rather than ALCC (Marlon et al., 2008; Power et al., 2008), other regional syntheses (e.g.`, Nevle & Bird, 2008; McWethy et al., 2009) show that biomass burning correlates strongly with the rise and fall of human societies.

6.5. FUTURE PERSPECTIVES AND CONCLUSIONS

Holocene carbon cycle modeling can be improved in multiple ways to achieve more accurate quantification of carbon balances throughout history. Differentiating among different types of land use systems (e.g. Ellis & Ramankutty, 2008; Verburg et al., 2009), would improve the quality of our carbon budget simulations by allowing us to simulate a more diverse suite of land use patterns (e.g., managed and unmanaged rangelands, managed forests). A future implementation of our ALCC model should have a spatially variable scheme for land rotation based on climate and soil fertility, so that in places where soils are exhausted more quickly people are forced to use more land, implementing, e.g., a short 3-5 year rotation-time shifting cultivation in the tropics. Also, accounting for improvements in technology (e.g., the development of irrigation or heavy steel plows) by having a spatially and temporally dynamic agricultural land suitability dataset would allow us to better simulate the spatial distributions of land use over time.

Running the DGVM with a transient Holocene climate scenario, either modeled or reconstructed, could help improve the realism of the simulations by accounting for the shifts in terrestrial C caused by climate change, e.g., following the Holocene development and subsequent collapse of the "green Sahara" or the advance and retreat of the polar timberline. Ultimately, when used in a coupled mode, our ALCC scenarios would allow investigation of feedbacks between climate, carbon and land use and the potential to address questions on human-induced irreversible ecosystem shifts caused by perturbations to the vegetation-climate system. Finally, a number of efforts are currently underway to improve the functionality of DGVMs to more accurately model global carbon exchanges, e.g., by including a representation of peatland dynamics or using more plant functional types. All of these improvements will help achieve more realistic modeling designs towards the central

goal of obtaining a more precise representation of past carbon cycles. This will contribute to a better understanding of the role of humans in the earth system and the present and future states of the global carbon cycle.

ALCC models that include land use intensification in response to population pressure and improvements in agricultural technologies (Ruddiman & Ellis, 2009) result in much higher estimates of ALCC and carbon release in prehistoric times than do studies that assume relatively constant per capita land use based on 20th century values. As a result, our estimates of ALCC-driven carbon emissions are substantially higher than previous studies. However, considering the range of estimates for carbon sequestration in peats during the Holocene, our ALCC emission estimates are compatible with the $\delta^{13}CO_2$ record, and allow us to explain Holocene carbon dynamics that cannot be attributed to other natural processes.

Carbon emissions as a result of anthropogenic land use over the preindustrial Holocene could have had a very substantial impact on the global carbon cycle. Even before 1000 BC (3 ka), up to 102 Pg of carbon could have been emitted into the atmosphere due to human land use. This amount of carbon could have contributed to, but cannot fully explain, the increase in atmospheric CO_2 in the mid-Holocene. By AD 1850, this amount increases to roughly 360 Pg, which equates to a ~25 ppm increase in atmospheric CO_2. In this sense, our results favor far larger early anthropogenic carbon emissions than previous estimates (which are a factor of 3-7 smaller). This is a substantial fraction of the amount posed in the original early anthropogenic hypothesis (Ruddiman, 2003). As a result, the world is much warmer than it would otherwise be.

Acknowledgements

This research was supported by grants from the Swiss National Science Foundation [PP0022_119049] and the Italian Ministry for Research and Education [FIRB RBID08LNFJ]. C.L. was supported by Deutsche Forschungsgemeinschaft (DFG, priority program Interdynamik SPP-1266). The authors thank Junmei Hu for assistance in interpreting Chinese population data, Navin Ramankutty for helpful discussions, and two anonymous reviewers, whose comments improved this manuscript.

References

Bazilevich, N. I., Rodin, L. Y. & Rozov, N. N. (1971) Geographical aspects of biological productivity. Soviet Geography: Review and Translation, 12, 293-317.

Bellwood, P. (2005) First Farmers: The Origins of Agricultural Societies, edn. Blackwell Publishing, Oxford.

Boserup, E. (1965) The Conditions of Agricultural Growth: The Economics of Agrarian Change Under Population Pressure, edn. Aldine, Chicago.

Boserup, E. (1981) Population and Technological Change: A Study of Long Term Trends, edn. University of Chicago Press, Chicago.

Boyle, J. F., Gaillard, M. J., Kaplan, J. O. & Dearing, J. A. (2010) Modelling prehistoric land use and carbon budgets: A critical review. The Holocene, 21(5).

Brovkin, V., Bendtsen, J., Claussen, M., Ganopolski, A., Kubatzki, C., Petoukhov, V. & Andreev, A. (2002) Carbon cycle, vegetation, and climate dynamics in the Holocene: Experiments with the CLIMBER-2 model. Global Biogeochemical Cycles, 16, doi:10.1029/2001GB001662.

Chao, K. (1986) Man and land in Chinese history: An economic analysis, edn. Stanford University Press.
Chepstow-Lustry, A. & Winfield, M. (2000) Inca agroforestry: Lessons from the past. Ambio, 29, 322-328.
Cook, O. F. (1921) Milpa agriculture, a primitive tropical system. Smithsonian Institution Annual Report, 1919, 307-326.
Cramer, W., Bondeau, A., Woodward, F. I., Prentice, C., Betts, R. A., Brovkin, V., Cox, P. M., Fisher, V., Foley, J. A., Friend, A. D., Kucharik, C., Lomas, M. R., Ramankutty, N., Sitch, S., Smith, B., White, A. & Young-Molling, C. (2001) Global response of terrestrial ecosystem structure and function to CO_2 and climate change: results from six dynamic global vegetation models. Global Change Biology, 7, 357-374.
de Beaulieu, J.-L., Miras, Y., Andrieu-Ponel, V. & Guiter, F. (2005) Vegetation dynamics in north-western Mediterranean regions: Instability of the Mediterranean bioclimate. Plant Biosystems, 139, 114-126.
Dearing, J. A. (2006) Climate-human-environment interactions: resolving our past. Climate of the Past, 2, 187-203.
Denevan, W. M. (1992) The Pristine Myth: The landscape of the Americas in 1492. Annals of the Association of American Geographers, 82, 369-385.
Dümenil Gates, L. & Ließ, S. (2001) Impacts of deforestation and afforestation in the Mediterranean region as simulated by the MPI atmospheric GCM. Global and Planetary Change, 30, 309-328.
Ellis, E. C. & Ramankutty, N. (2008) Putting people in the map: anthropogenic biomes of the world. Frontiers in Ecology and the Environment, 6, 439-447.
Ellis, E. C. & Wang, S. M. (1997) Sustainable traditional agriculture in the Tai Lake region of China. Agricultural Systems and Environment, 61, 177-193.
Elsig, J., Schmitt, J., Leuenberger, D., Schneider, R., Ever, M., Leuenberger, F., Joos, F., Ficher, H. & Stocker, T. (2009) Stable isotope constraints on Holocene carbon cycle changes from an Antarctic ice core. Nature, 461, 507-510.
Ervynck, A., Lentacker, A., Müldner, G., Richards, M. & Dobney, K. (2007) An investigation into the transition from forest dwelling pigs to farm animals in medieval Flanders, Belgium. Pigs and Humans: 10,000 Years of Interaction (ed. by U. Albarella & K. Dobney & A. Ervynck), pp 171-193. Oxford University Press, Oxford.
Frolking, S. & Roulet, N. T. (2007) Holocene radiative forcing impact of northern peatland carbon accumulation and methane emissions. Global Change Biology, 13, 1079-1088.
Gaillard, M.-J., Suguita, S., Mazier, F., Kaplan, J. O., Trondman, A.-K., Broström, A., Hickler, T., Kjellström, E., Kuneš, P., Lemmen, C., Olofsson, J., Smith, B. & Strandberg, G. (2010) Holocene land-cover reconstructions for studies on land cover-climate feedbacks. Climate of the Past Discussions, 6, 307-346.
Gajewski, K., Viau, A., Sawada, M., Atkinson, D. & Wilson, S. (2001) Sphagnum peatland distribution in North America and Eurasia during the past 21,000 years. Global Biogeochemical Cycles, 15, 297-310.
Gorham, E. (1991) Northern peatlands: role in the carbon cycle and probable responses to climatic warming. Ecological Applications, 1, 182-195.
Grove, A. T. & Rackham, O. (2001a) Natural Vegetation in Historic Times. The Nature of Mediterranean Europe: An Ecological History (ed. by J. Havell), pp 167-189. Yale University Press, New Haven.
Grove, A. T. & Rackham, O. (2001b) The Nature of Mediterranean Europe: An Ecological History, edn. Yale University Press, New Haven and London.
Hellman, S. E. V., Gaillard, M.-J., Bröstrom, A. & Sugita, S. (2008) Effects of the sampling design and selection of parameter values on pollen-based quantitative reconstructions of regional vegetation: A case study in southern Sweden using the REVEALS model. Vegetation History and Archaeobotany, 17, 445-459.

Hermy, M. & Verheyen, K. (2007) Legacies of the past in the present-day forest biodiversity: a review of past land-use effects on forest plant species composition and diversity. Ecological Research, 22, 361-371.

Hoelzmann, P., Jolly, D., Harrison, S. P., Laarif, F., Bonnefille, R. & Pachur, H. J. (1998) Mid-Holocene land-surface conditions in northern Africa and the Arabian Peninsula: A data set for the analysis of biogeophysical feedbacks in the climate system. Global Biogeochemical Cycles, 12, 35-51.

Houghton, J. T., Hackler, J. L. & Lawrence, K. T. (1999) The U.S. carbon budget: Contributions from land-use change. Science, 285, 574-578.

Houghton, R. A. (2003) Revised estimates of the annual net flux of carbon to the atmosphere from changes in land use and land management 1850-2000. Tellus, 55B, 378-390.

Johnston, K. J. (2003) The intensification of pre-industrial cereal agriculture in the tropics: Boserup, cultivation lengthening, and the Classic Maya. Journal of Anthropological Archaeology, 22, 126-161.

Joos, F., Gerber, S., Prentice, I. C., Otto-Bliesner, B. L. & Valdes, P. (2004) Transient simulations of Holocene atmospheric carbon dioxide and terrestrial carbon since the last glacial maximum. Global Biogeochemical Cycles, 18, GB2002 10.1029/2003GB002156.

Jung, M., Vetter, M., Herold, M., Churkina, G., Reichstein, M., Zaehle, S., Ciais, P., Viovy, N., Bondeau, A., Chen, Y., Trusilova, K., Feser, F. & Heimann, M. (2007) Uncertainties of modeling gross primary productivity over Europe: A systematic study on the effects of using different drivers and terrestrial biosphere models. Global Biogeochemical Cycles, 21, doi:10.1029/2006GB002915.

Kaplan, J. O. (2001) Geophysical Applications of Vegetation Modeling. Department of Ecology, pp 132. Lund University, Lund.

Kaplan, J. O., Krumhardt, K. M. & Zimmerman, N. (2009) The prehistorical and preindustrial deforestation of Europe. Quaternary Science Reviews, 28, 3016-3034.

Kaplan, J. O., Prentice, I. C., Knorr, W. & Valdes, P. J. (2002) Modeling the dynamics of terrestrial carbon storage since the Last Glacial Maximum. Geophysical Research Letters, 29.

Klein Goldewijk, K. (2001) Estimating global land use change over the past 300 years: The HYDE Database. Global Biogeochemical Cycles, 15, 417 - 433.

Klein Goldewijk, K., Beusen, A. & Janssen, P. (2010) Long term dynamic modeling of global population and built-up area in a spatially explicit way, HYDE 3 .1. The Holocene, 20(4), 565-573.

Klein Goldewijk, K., Beusen, A., van Drecht, G. & de Vos, M. (2011) The HYDE 3.1 spatially explicit database of human induced global land use change over the past 12,000 years. Global Ecology & Biogeography, 20(1): 73-86.

Krumhardt, K. M. (2010) ARVE Technical Report #3: Methodology for worldwide population estimates: 1000 BC to 1850. École Polytechnique Fédérale de Lausanne, Dept. of Environmental Engineering, ARVE Research Group.

Krumhardt, K. M. & Kaplan, J. O. (2010) ARVE Technical Report #2: A spline fit to atmospheric CO_2 records from Antarctic ice cores and measured concentrations for the past 25,000 years. Environmental Engineering Institute, Ecole Polytechnique Fédérale de Lausanne.

Lemmen, C. (2009) World distribution of land cover changes during Pre- and Protohistoric times and estimation of induced carbon releases. Géomorphologie : relief, processus, environnement, 4/2009, 303-312.

MacDonald, G. M., Beilman, D. W., Kremenetski, K. V., Sheng, Y., Smith, L. C. & Velichko, A. A. (2006) Rapid early development of circumarctic peatlands and atmospheric CH4 and CO_2 variations. Science, 314, 285-288.

MacFarling Meure, C., Etheridge, D. M., Trudinger, C., Steele, L. P., Langenfelds, R. L., van Ommen, T., Smith, A. & Elkins, J. (2006) The Law Dome CO_2, CH_4, and N_2O ice core records extended to 2000 year BP. Geophysical Research Letters, 33, L14810 10.1029/2006GL026152.

Marlon, J. R., Bartlein, P. J., Carcaillet, C., Gavin, D. G., Harrison, S. P., Higuera, K., Joos, F., Power, M. J. & Prentice, I. C. (2008) Climate and human influences on global biomass burning over the past two millennia. Nature Geoscience, 1, 697-702.

Mathey, R. T. & Gurr, D. L. (1983) Variation in prehistoric agricultural systems of the New World. Annual Review of Anthropology, 12, 79-103.

Mazoyer, M. & Roudart, L. (2006) A History of World Agriculture, edn. Earthscan, London.

McEvedy, C. & Jones, R. (1978) Atlas of World Population History, edn. Penguin, London.

McGuire, A. D., Sitch, S., Clein, J. S., Dargaville, R., Esser, G., Foley, J., Heimann, M., Joos, F., Kaplan, J., Kicklighter, D. W., Meier, R. A., Melillo, J. M., Moore, B., Prentice, I. C., Ramankutty, N., Reichenau, T., Schloss, A., Tian, H., Williams, L. J. & Wittenberg, U. (2001) Carbon balance of the terrestrial biosphere in the twentieth century: Analyses of CO_2, climate and land use effects with four process-based ecosystem models. Global Biogeochemical Cycles, 15, 183-206.

McWethy, D. B., Whitlock, C., Wilmshurst, J. M., McGlone, M. S. & Li, X. (2009) Rapid deforestation of South Island, New Zealand, by early Polynesian fires. The Holocene, 19.

Nevle, R. J. & Bird, D. K. (2008) Effects of syn-pandenic fire reduction and reforestation in the tropical Americas on atmospheric CO_2 during European conquest. Palaeogeography, Palaeoclimatology, Palaeoecology, 264, 25-38.

Olofsson, J. & Hickler, T. (2008) Effects of human land-use on the global carbon cycle during the last 6,000 years. Vegetation History and Archaeobotany, 17, 605-615.

Olson, J. S., Watts, J. A. & Allison, J. (1983) Carbon in live vegetation of major world ecosystems, ORNL 5862, Environmental Sciences Division Publ. No. 1997, edn. Oak Ridge National Library, Oak Ridge, Tennessee.

Pitman, A. J., De Noblet-Ducoudre, N., Cruz, F. T., Davin, E. L., Bonan, G. B., Brovkin, V., Claussen, M., Delire, C., Ganzeveld, L., Gayler, V., Van Den Hurk, B. J. J. M., Lawrence, P. J., Van Der Molen, M. K., Mueller, C., Reick, C. H., Seneviratne, S. I., Strengen, B. J. & Voldoire, A. (2009) Uncertainties in climate responses to past land cover change: First results from the LUCID intercomparison study. Geophysical Research Letters, 36.

Pohl, M. D., Pope, K. O., Jones, J. G., Jacob, J. S., Piperno, D. R., deFrance, S. D., Lentz, D. L., Gifford, J. A., Danforth, M. E. & Josserand, J. K. (1996) Early Agriculture in the Maya Lowlands. Latin American Antiquity, 7, 355-372.

Pongratz, J., Reick, C., Raddatz, T. & Claussen, M. (2008) A reconstruction of global agricultural areas and land cover for the last millennium. Global Biogeochemical Cycles, 22, doi:10.1029/2007GB003153.

Power, M., Marlon, J., Ortiz, N., Bartlein, P., Harrison, S., Mayle, F., Ballouche, A., Bradshaw, R., Carcaillet, C., Cordova, C., Mooney, S., Moreno, P., Prentice, I., Thonicke, K., Tinner, W., Whitlock, C., Zhang, Y., Zhao, Y., Ali, A., Anderson, R., Beer, R., Behling, H., Briles, C., Brown, K., Brunelle, A., Bush, M., Camill, P., Chu, G., Clark, J., Colombaroli, D., Connor, S., Daniau, A. L., Daniels, M., Dodson, J., Doughty, E., Edwards, M., Finsinger, W., Foster, D., Frechette, J., Gaillard, M. J., Gavin, D., Gobet, E., Haberle, S., Hallett, D., Higuera, P., Hope, G., Horn, S., Inoue, J., Kaltenrieder, P., Kennedy, L., Kong, Z., Larsen, C., Long, C., Lynch, J., Lynch, E., McGlone, M., Meeks, S., Mensing, S., Meyer, G., Minckley, T., Mohr, J., Nelson, D., New, J., Newnham, R., Noti, R., Oswald, W., Pierce, J., Richard, P., Rowe, C., Sanchez Goñi, M., Shuman, B., Takahara, H., Toney, J., Turney, C., Urrego-Sanchez, D., Umbanhowar, C., Vandergoes, M., Vanniere, B., Vescovi, E., Walsh, M., Wang, X., Williams, N., Wilmshurst, J. & Zhang, J. (2008) Changes in fire regimes since the Last Glacial Maximum: an assessment based on a global synthesis and analysis of charcoal data. Climate Dynamics, 30, 887-907.

Ramankutty, N. & Foley, J. (1998) Characterizing patterns of global land use: An analysis of global croplands data. Global Biogeochemical Cycles, 12, 667-685.

Ramankutty, N. & Foley, J. A. (1999) Estimating historical changes in global land cover: Croplands from 1700 to 1992. Global Biogeochemical Cycles, 13, 997-1027.

Ramankutty, N., Foley, J. A., Norman, J. & McSweeney, K. (2002) The global distribution of cultivatable lands: current patterns and sensitivity to possible climate change. Global Ecology & Biogeography, 11, 377-392.
Reina, R. E. (1967) Milpas and milperos: Implications for prehistoric times. American Anthropologist, New Series, 69, 1-20.
Ren, G. (2000) Decline of the mid- to late Holocene forests in China: Climatic change or human impact. Journal of Quaternary Science, 15, 273-281.
Richerson, P. J., Boyd, R. & Bettinger, R. L. (2001) Was agriculture possible during the Pleistocene but mandatory during the Holocene? A climate change hypothesis. American Antiquity, 66, 387-411.
Ruddiman, W. F. (2003) The anthropogenic greenhouse era began thousands of years ago. Climatic Change, 61, 261-293.
Ruddiman, W. F. (2005) Plows, Plagues, and Petroleum: How Humans Took Control of the Climate, edn. Princeton University Press, Princeton.
Ruddiman, W. F. (2007) The Early Anthropogenic Hypothesis: Challenges and responses. Reviews of Geophysics, 45, doi:10.1029/2006RG000207.
Ruddiman, W. F. & Ellis, E. C. (2009) Effect of per-capita land-use changes on Holocene forest clearance and CO_2 emissions. Quaternary Science Reviews, 28, 3011-3015.
Ruddiman, W. F., Vavrus, S. J. & Kutzbach, J. E. (in press) Can natural or anthropogenic explanations of early Holocene CO_2 and CH_4 increases be falsified? The Holocene.
Sitch, S., Smith, B., Prentice, I. C., Arneth, A., Bondeau, A., Cramer, W., Kaplan, J. O., Levis, S., Lucht, W., Sykes, M. T., Thonicke, K. & Venevsky, S. (2003) Evaluation of ecosystem dynamics, plant geography and terrestrial carbon cycling in the LPJ dynamic global vegetation model. Global Change Biology, 9, 161-185.
Strassmann, K. M., Joos, F. & Fischer, G. (2008) Simulating effects of land use changes on carbon fluxes: past contributions to atmospheric CO_2 increases and future commitments due to losses of terrestrial sink capacity. Tellus, 60B, 583-603.
Sugita, S. (2007a) Theory of quantitative reconstruction of vegetation I: Pollen from large sites REVEALS regional vegetation. Holocene, 17, 229-241.
Sugita, S. (2007b) Theory of quantitative reconstruction of vegetation II: All you need is LOVE. Holocene, 17, 243-257.
Takata, K., Saito, K. & Yasunari, T. (2009) Changes in the Asian monsoon climate during 1700-1850 induced by preindustrial cultivation. PNAS, 106, 9586-9589.
Tinner, W., Nielsen, E. H. & Lotter, A. F. (2007) Mesolithic agriculture in Switzerland? A critical review of the evidence. Quaternary Science Reviews, 26, 1416-1431.
Tinner, W., van Leeuwen, J. F. N., Colombaroli, D., Vescovi, E., Van der Knaap, W. O., Henne, P. D., Pasta, S., D'Angelo, S. & La Mantia, T. (2009) Holocene environmental and climatic changes at Gorgo Basso, a coastal lake in southern Sicily, Italy. Quaternary Science Reviews, 28, 1498-1510.
Van der Knaap, W. O. & van Leeuwen, J. F. N. (1995) Holocene vegetation succession and degradation as responses to climatic change and human activity in the Serra de Estrela, Portugal. Review of Palaeobotany and Palynology, 89, 153-211.
Verburg, P. H., van de Steeg, J., Veldkamp, A. & Willemen, L. (2009) From land cover change to land function dynamics: A major challenge to improve land characterization. Journal of Environmental Management, 90, 1327-1335.
Verheyen, K., Bossuyt, B., Hermy, M. & Tack, G. (1999) The land use history (1278-1990) of a mixed hardwood forest in western Belgium and its relationship with chemical soil characteristics. Journal of Biogeography, 26, 1115-1128.
Wanner, H., Beer, J., Bütikofer, J., Crowley, T. J., Cubasch, U., Flückiger, J., Goosse, H., Grosjean, M., Joos, F., Kaplan, J. O., Küttel, M., Müller, S. A., Prentice, I. C., Solomina, O., Stocker, T. F., Tarasov, P., Wagner, M. & Widmann, M. (2008) Mid- to Late Holocene climate change: An overview. Quaternary Science Reviews, 27, 1791-1828.

Weninger, B., Alram-Stern, E., Bauer, E., Clare, L., Danzeglocke, U., Joris, O., Claudia, K. E., Gary, R. F., Todorova, H. & van Andel, T. (2006) Climate forcing due to the 8200 cal yr BP event observed at Early Neolithic sites in the eastern Mediterranean. Quaternary Research, 66, 401-420.

Wilken, G. C. (1971) Food-producing systems available to the ancient Maya. American Antiquity, 36, 432-448.

Williams, M. (2008) A new look at global forest histories of land clearing. Annual Review of Environment and Resources, 33, 345-367.

Yu, Z. (2011) Holocene carbon flux histories of the world's peatlands: Global carbon-cycle implications, The Holocene, 21(5), 761-774.

Zhao, W. & Xie, S. (1988) History of Population in China (Zhongguo Ren Kou Shi), Ist edition edn. People's Publishing House, Beijing.

Zimmermann, A., Richter, J., Frank, T. & Wendt, K.-P. (2004) Landschaftsarchäologie II - Überlegungen zu Prinzipien einer Landschaftsarchäologie. Berichte der Römisch-Germanischen Komission, 85, 37-96.

Supplementary material to the manuscript: Holocene carbon emissions as a result of anthropogenic land cover change

By Jed O. Kaplan *et al*.

1. Detailed methods description

In order to quantify ALCC emissions over the Holocene we 1) developed a new scenario of global ALCC from 8 ka cal. BP (calendar years before AD 1950) to AD 1850 based on existing methodology, 2) assembled climate, soils and CO_2 data used to drive a Dynamic Global Vegetation Model (DGVM), 3) modified the LPJ DGVM to handle ALCC and made several other small improvements to the model, and 4) ran the model in a number of experiments to characterize the range of possible emissions scenarios. Development of the new ALCC time series involved preparation of a new database of estimates of prehistoric and historical global population. We assembled new driver datasets of CO_2 concentrations and meteorology based on the latest available datasets. The modifications to the LPJ DGVM included a novel mechanism to simulate transient ALCC and shifting cultivation and an improved geographic distribution of soil organic matter based on compilation of observations.

1.1 *Population data before 3 ka*

In this model, the adaptive co-evolution of socio-technological traits and population growth rate from foraging to agro-pastoral societies is simulated. GLUES simulates human population in 685 regions (figure S1), with a growth rate that changes with time and the rate of expansion of both agricultural subsistence and technology. Between 8 ka and 3 ka, the modeled mean doubling time for global human population is 2500 years, and ranges from 1721 to 6495 years. Population growth accelerates fastest during the transition to agriculture in western Eurasia and East Asia. At 3 ka, global population simulated by GLUES is in reasonable agreement with the independent record of population we assembled for this time period based on historical estimates. To distribute the global values simulated by GLUES geographically, we scaled each region's population at 3 ka in our historical dataset by the simulated fractional change in GLUES simulated global population relative to 3 ka.

1.2 *Climate and soils driver data for LPJ*

The LPJ DGVM is driven by spatially and temporally explicit datasets of climate, soil properties and atmospheric CO_2 concentrations (Sitch *et al.*, 2003). LPJ requires a timeseries of climate data to run; to realistically simulate vegetation dynamics it is not sufficient to use climatological mean forcing. As the primary purpose of this study is to quantify the role of ALCC on the terrestrial carbon cycle, and because realistic global paleoclimate forcing datasets are currently unavailable, either from climate models or based on proxy reconstructions, we used a standard 20^{th} century observation-based climate dataset to run LPJ; a 100-year long timeseries of global climate (monthly mean temperature and cloud cover, monthly total precipitation) gridded at 30' resolution.

The climate dataset is a combination of the CRU TS 3.00 1900-2006 high-resolution gridded climate time series (based on Mitchell & Jones, 2005) with the WorldClim 1.4 climatology (Hijmans *et al.*, 2005). This hybrid climate dataset has the advantage of being more realistic than the original CRU TS 3.00 data. In particular, the CRU dataset is based on the outdated ETOPO5 digital elevation model (DEM), while WorldClim uses an SRTM-based DEM; WorldClim also has a more realistic spatial representation of precipitation patterns in the tropics, as the dataset is based on many more precipitation stations than CRU. We extracted the 100-year time period from 1906-2005 from CRU TS 3.00, as the data for 2006 are incomplete and the earliest years of the time-series are simply relaxed to the 1961-1990 mean for many parts of the world, especially in the tropics. We created anomalies (absolute for temperature, relative fractions for cloud and precipitation) between CRU TS 3.00 and its 1961-1990 mean and applied these anomalies to a 30' version of the WorldClim 1.4 climatology. We experimented with detrending the CRU TS 3.00 data to remove any 20th century long-term trend in climate, but found that for most places the slope of the regression line through the data was not significantly different from zero, and that the resulting detrended data often resulted in a reduction in the magnitude of interannual variability. Therefore, we used the raw anomalies from CRU to construct our climate time series.

LPJ requires information on the soil physical properties available water holding capacity (AWC) and saturated hydraulic conductivity (K_{sat}). We further used data on total soil clay content to define partitioning between soil organic matter pools (described in sections below). The soils data we used are based primarily on the ISRIC-WISE derived soil properties on a 5 by 5 arc-minutes global grid (ver. 1.1), which is itself a product of the FAO Soil Map of the World, newer large-scale soil maps for certain countries and continents, and taxo-transfer databases based on the WISE pedon libraries (Batjes, 2006). AWC and K_{sat} are a function of soil texture fractions, bulk density, and coarse fragment content contained in the ISRIC-WISE dataset and were calculated using pedotransfer functions described in Melton et al. (2010). The ISRIC-WISE dataset contains information on soil properties for a maximum of five evenly spaced (20 cm) depth levels in the top 1 m of the soil. Where typical soil profiles indicate that the soil is shallower than 1m, the ISRIC-WISE database provides information only for those depth levels above bedrock. We converted fractional AWC calculated using the pedotransfer functions to a gross volumetric AWC for the two layers used by the LPJ soil hydrology scheme (0-30 cm, 30 cm-bedrock) by multiplying by the minimum soil depth implied either by the ISRIC-WISE database or a separate map of soil effective rooting depth based on the typical maximum rooting depth for a mapping unit defined in the FAO Digital Soil Map of the World (FAO, 1995).

1.3 *Modifications to the LPJ DGVM*

We used the version of LPJ described in Sitch et al., (2003) with the following modifications: 1) we made a number of small modifications to the way surface downwelling shortwave radiation is calculated, including a provision to account for changes in the Earth's orbit with time, 2) we changed the way the partitioning of the flux to the soil organic matter (SOM) pools is determined, 3) we modified the controls on SOM decomposition in the slow soil pool, and 4) we implemented a scheme for simulating the effects of ALCC on the landscape (described in section 2.3 of this chapter).

To model the changing magnitude and seasonality of top-of-the-atmosphere (TOA) solar forcing, we replaced the simple insolation calculation in the standard LPJ with a module that follows Berger (1978). This module is driven by calendar year, latitude, and the solar constant and allows accurate calculation of TOA insolation at any year and any latitude in the range ±1000 ka. We expect the direct effect of variability in TOA insolation on vegetation to have been small compared to the way insolation changes over the Holocene affected the Earth's radiative budget and therefore the climate system (Wanner *et al.*, 2008). Outside of the tropics, where Holocene insolation variations were small, most terrestrial ecosystems are not generally light limited, moisture or temperature being more important (Churkina & Running, 1998; Nemani *et al.*, 2003). Nevertheless, the increased summertime insolation in high northern latitudes at the mid-Holocene relative to the present could have enhanced plant growth, especially in light-limited regions of northwestern Europe and southeastern China.

In evaluating the global spatial distribution of SOM in the standard version of LPJ, we noticed that almost all SOM was concentrated in high latitudes and mountains, with the greatest concentration of SOM found in cold, dry places, such as the Altai and Sayan mountains in Siberia. This is because in the standard LPJ, all SOM dynamics are a function of a baseline rate of microbial respiration, adjusted by an Arrhenius function for temperature and a linear function for soil moisture (Sitch *et al.*, 2003), with cold, dry conditions resulting in the lowest rates of decomposition. Recent studies of global SOM distribution in upland soils have shown that significantly more SOM may be found outside of boreal regions, e.g., in deep tropical and subtropical soils (Jobbágy & Jackson, 2000). Jobbágy & Jackson (2000) hypothesize that long-term storage of SOM is related to soil clay content and the stabilization of recalcitrant SOM in clay minerals. In order to improve LPJ's representation of the spatial distribution of SOM to better reconcile with observations, we modified the SOM partitioning and scheme in LPJ in three ways: 1) we adjusted the depth of the soil column for calculating organic matter content to 3 m unless shallower soils were classified in the input soil data set (see above for details) 2) we changed the partitioning of inputs between the fast and slow SOM pools, and 3) we removed the temperature and moisture modifiers to slow pool SOM decomposition. In standard LPJ, decomposing litter is partitioned between fast and slow SOM pools with a fixed ratio (1.5% to the slow pool). Our new scheme partitions litter input dynamically, based on the total amount of clay in the soil column, following

$$F_{slow} = F_{max} M_{clay} / 300 \qquad (2)$$

where F_{slow} is the fraction of decomposing litter entering the slow SOM pool, F_{max} is the maximum partitioning fraction (15%) and M_{clay} is the total mass of clay (kg m^{-2}) in the top 3m of the soil column (or less if shallower soil is specified in the soil input dataset). Under conditions of maximum clay content – ca. 300 kg m^{-2} is the maximum in our driver dataset – up to 15% of the decomposed litter is directed to the slow pool. We also removed the temperature and moisture modifiers to the baseline respiration rate for the slow SOM pool to acknowledge recent evidence that has suggested that microbial decomposition of recalcitrant SOM has very low sensitivity to changes in environmental conditions (Davidson & Janssens, 2006). The resulting map of global SOM content agrees well with the biome-

based classification of Jobbágy & Jackson (2000), and with standard meteorology and soils forcing, results in a global SOM store at equilibrium of 2300-2400 Pg.

References

Batjes, N.H. (2006) ISRIC-WISE derived soil properties on a 5 by 5 arc-minutes global grid. In: *Report 2006/02 (available through: http://www.isric.org), ISRIC- World Soil Information* Wageningen.

Berger, A. (1978) Long-term variations of caloric insolation resulting from the Earth's orbital elements. *Quaternary Research*, **9**, 139-167.

Churkina, G. & Running, S.W. (1998) Constrasting climatic controls on the estimated productivity of global terrestrial biomes. *Ecosystems*, **1**, 206-215.

Davidson, E.A. & Janssens, I.A. (2006) Temperature sensitivity of soil carbon decomposition and feedbacks to climate change. *Nature*, **440**, 165-173.

FAO (1995) *Digital Soil Map of the World*. Available at: (accessed

Hijmans, R.J., Cameron, S.E., Parra, J.L., Jones, P.G. & Jarvis, A. (2005) Very high resolution interpolated climate surfaces for global land areas. *International Journal of Climatology*, **25**, 1965-1978.

Jobbágy, E.G. & Jackson, R.B. (2000) The vertical distribution of soil organic carbon and its relation to climate and vegetation. *Ecological Applications*, **10**, 423-436.

Melton, J.R., Kaplan, J.O., Pfeiffer, M. & Collins, P.M. (2010) Documentation of the ARVE Dynamic Global Vegetation Model (ARVE-DGVM). In. Environmental Engineering Institute, Ecole Polytechnique Fédérale de Lausanne

Mitchell, T.D. & Jones, P.D. (2005) An improved method of constructing a database of monthly climate observations and associated high-resolution grids. *International Journal of Climatology*, **25**, 693-712.

Nemani, R.R., Keeling, C.D., Hashimoto, H., Jolly, W.M., Piper, S.C., Tucker, C.J., Myneni, R.B. & Running, S.W. (2003) Climate-driven increases in global terrestrial net primary production from 1982 to 1999. *Science*, **300**, 1560-1563.

Ruddiman, W.F. (2007) The Early Anthropogenic Hypothesis: Challenges and responses. *Reviews of Geophysics*, **45**, doi:10.1029/2006RG000207.

Sitch, S., Smith, B., Prentice, I.C., Arneth, A., Bondeau, A., Cramer, W., Kaplan, J.O., Levis, S., Lucht, W., Sykes, M.T., Thonicke, K. & Venevsky, S. (2003) Evaluation of ecosystem dynamics, plant geography and terrestrial carbon cycling in the LPJ dynamic global vegetation model. *Global Change Biology*, **9**, 161-185.

Wanner, H., Beer, J., Bütikofer, J., Crowley, T.J., Cubasch, U., Flückiger, J., Goosse, H., Grosjean, M., Joos, F., Kaplan, J.O., Küttel, M., Müller, S.A., Prentice, I.C., Solomina, O., Stocker, T.F., Tarasov, P., Wagner, M. & Widmann, M. (2008) Mid- to Late Holocene climate change: An overview. *Quaternary Science Reviews*, **27**, 1791-1828.

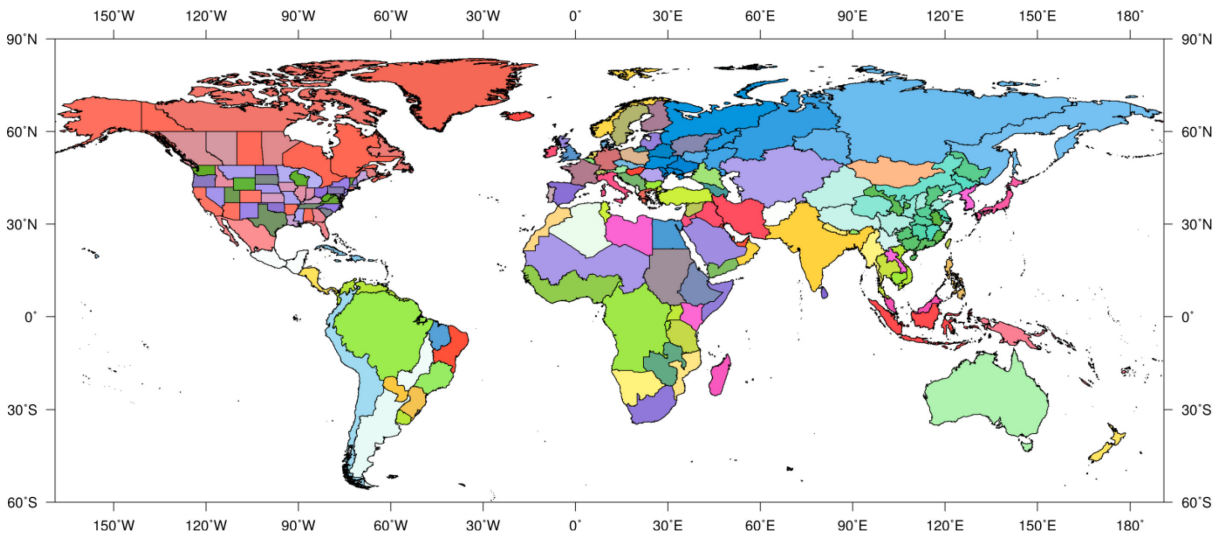

Figure S1. Administrative units used in this study.

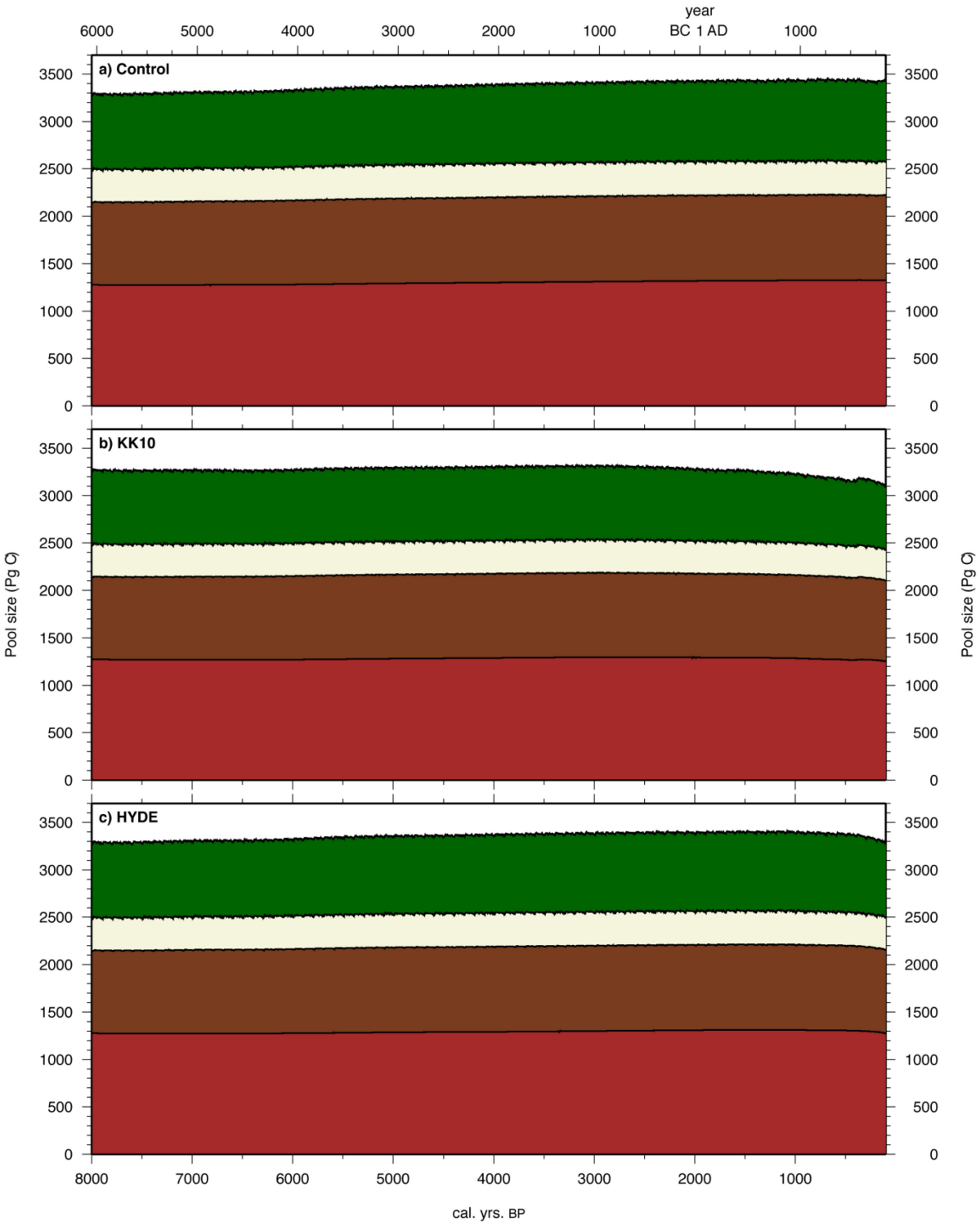

Figure S2. Different carbon pool sizes for the Control and the two LU scenarios.

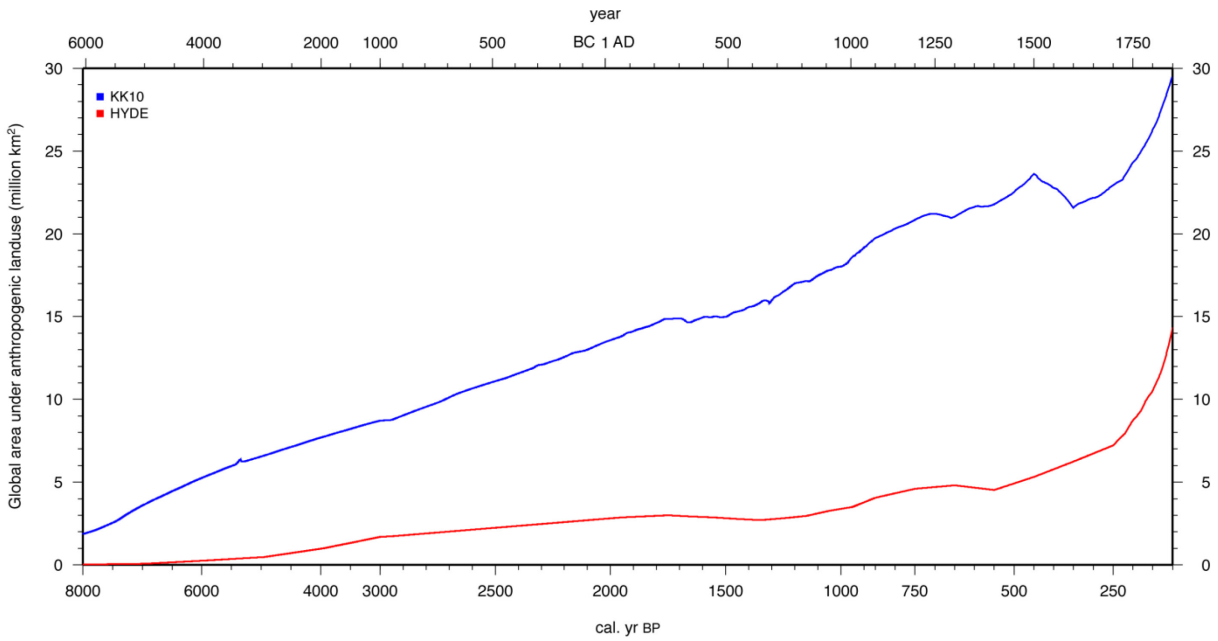

Figure S3. Global anthropogenic land use development under the two different scenarios.